TOWARD A MICROFLUIDIC PLATFORM FOR CELL FREE SYNTHESIS OF MORPHINE DEGRADATION PATHWAY ENZYMES

A Thesis

Presented to the Faculty of the Graduate School

of Cornell University

in Partial Fulfillment of the Requirements for the Degree of

Master of Science

by

Sandra Vadhin

December 2020

ABSTRACT

Opioids are a class of drugs highly valued for their potent analgesic properties; however, they are also highly addictive and cause severe side effects. Alternative manufacturing methods may be the disruption needed to overcome the cost and availability issues associated with naloxone, the opioid overdose antidote. Toward this need, we propose the development of a biosynthetic route of naloxone production with morphine as the precursor. In this work, we produced morphine dehydrogenase - an enzyme that catalyzes the oxidation of morphine to morphinone - by cell free protein synthesis (CFPS), taking advantage of the speed of CFPS compared to cell-based culture. To supplement our constraint-based metabolic modeling and detect compounds of interest with rigor, we developed a method for absolute quantification of metabolites and nucleotide sugars by reversed-phase liquid chromatography-mass spectrometry. Finally, we have characterized and begun modeling a microreactor with an eye toward its future use as our main bioprocessing platform. Taken together, we have developed a rapid protocol for expression of what could serve as the first enzyme in a novel biosynthetic pathway and laid the groundwork for reactor optimization.

BIOGRAPHICAL SKETCH

Sandra Vadhin received her secondary education at public and public charter schools of the Los Angeles Unified School District. She attended the University of California, Riverside and graduated *cum laude* in 2018 with a Bachelor of Science in Bioengineering. In August 2018, she began graduate studies in the Robert Frederick Smith School of Chemical and Biomolecular Engineering at Cornell University where she joined Professor Jeffrey Varner's research group.

This work is dedicated to my dad, Sucha Vadhin.

ACKNOWLEDGEMENTS

I would like to begin by thanking my mom Lisa and my brother Bryan for their love and support. It goes without saying that I would like to thank Professor Jeffrey D. Varner for his patience and guidance in my development as an scientist. Many, many thanks are due Dr. Michael Vilkhovoy for his patience and graciousness as he trained me. For their valued advice, I would like to thank past and senior Varner Lab members: Dr. David Dai, Dr. Nicholas Horvath, Kritika Kashyap, Dr. Rachel LeCover, and Zhiping Zhang. To Sruti Dammalapati, Zhihao Feng, Anirudh Murali Narayanan, Abhishek Murti, Aasim Ayaz Wani, and my lab twin Abhinav Adhikari, thank you for being awesome and positive colleagues. Finally, I would like to thank Noya Achiasaf, Lisa Durand, Jennifer Fineman, Yaeir Halfon, Elena Villaescusa Pineda, Josiah Wong, and Julia Zaytsev for their encouragement and 10+ years of friendship.

TABLE OF CONTENTS

LIST OF TABLES

LIST OF FIGURES

CHAPTER 1

INTRODUCTION

1.1 Evolution of cell free protein synthesis

[1] Cell free biology is an emerging technology for research, and the point of care manufacturing of a wide array of macromolecular and small molecule products. A distinctive feature of cell free systems is the absence of cellular growth and maintenance, thereby allowing the direct allocation of carbon and energy resources toward a product of interest. Moreover, cell free systems are more amenable than living systems to observation and manipulation, hence allowing rapid tuning of reaction conditions. Recent advances in cell free extract preparation and energy regeneration mechanisms have increased the versatility and range of applications that can be produced cell free. Thus, the cell free platform has transformed from merely an investigative research tool to become a promising alternative to traditionally used living systems for biomanufacturing as well as biological research. In combination with the rise of synthetic biology, cell free systems today have not only taken on a new role as a promising technology for just in time manufacturing of therapeutically important biologics and high-value small molecules, but have also been utilized for applications such as biosensing, prototyping genetic parts, and metabolic engineering. They have also been used as educational tools at the high school and undergraduate levels for understanding synthetic biology due to their ease of use, rapid response times, and the availability of commercial kits for different cell free platforms in-

[1] Adapted with permission from Vilkhovoy, M.; Adhikari, A.; Vadhin, S.; Varner, J. D. The Evolution of Cell Free Biomanufacturing. Processes 2020, 8 (6), 675. https://doi.org/10.3390/pr8060675.

cluding *E. coli*, Chinese Hamster Ovary (CHO), HeLa, and plant cells [4, 30, 55]. Thus, cell free technologies are promising tools that will likely be at the center of many future synthetic biology applications.

Arguably, today the most widely used cell free technology is cell free protein synthesis (CFPS), an *in vitro* platform for protein transcription (TX) and translation (TL). The role of CFPS in research is not new (Fig. 1.1); cell free systems have been used for decades to explore fundamental biological mechanisms. For example, some of the first uses of CFPS were in the 1950s by Borsook [15] and Winnick [186] who used animal tissue homogenates to study how amino acids were incorporated into proteins. A few years later, *Staphylococcus aureus* extracts were used to confirm amino acid incorporation [47]. In 1956, the role of adenosine triphosphate (ATP) in protein production was discovered using rat liver extracts [68], and Nirenberg and Matthaei [105, 122] demonstrated templated translation i.e., the now familiar codon code, using *E. coli* cell free extracts (this work later led to a Nobel Prize in 1968). What arguably could be recognized as the first precursor to modern cell free transcription and translation applications was developed in 1967 by Lederman and Zubay [95]; they developed a coupled transcription-translation bacterial extract that allowed DNA to be used as a template. Shortly after, Spirin and coworkers improved cell free extract protein production with a continuous exchange of reactants and products, allowing the system to run for tens of hours; however, these systems could only synthesize a single product and were energy limited [159]. More recently, energy efficiency of *E. coli* CFPS was improved by generating ATP with substrate level phosphorylation [90] and oxidative phosphorylation in the Cytomim system [82, 83, 80]. The use of glucose as an energy source was also explored [20]. Since oxidative phosphorylation is a membrane associated process, the study of

Swartz and colleagues revealed that membrane dependent energy metabolism can be activated in a cell free system, suggesting complex metabolism is still occurring. Another platform, myTXTL [48], uses a different metabolic process that couples ATP regeneration and inorganic phosphate recycling to extend the duration of protein production. Synthetic genetic circuitry can also be constructed to control gene expression using a variety of approaches. Bacteriophage RNA polymerases are commonly used in CFPS for transcription. However, the use of a vast array of bacterial regulatory elements based on the sigma factor family has recently been explored, allowing multi-layer genetic cascades to be easily implemented [148, 150, 48]. Lastly, cell free systems have also been used as educational tools, at the high school and undergraduate levels, for understanding synthetic biology owing to their ease of use and rapid response times [4, 30]. Commercial kits are available for research and educational applications generated from different organisms, including *E. coli*, Chinese Hamster Ovary (CHO), HeLa, and plant cells [55]. Thus, the developments in CFPS have expanded its repertoire of applications, enabling it as a viable alternative to living systems for not only investigative research but also bioengineering and biomanufacturing on both small and large scales.

In this review, we discuss the evolution of cell free technologies, particularly, advancements in extract preparation, cell free protein synthesis and cell free metabolic engineering applications. We then conclude with a discussion of the mathematical modeling of cell free systems. Mathematical modeling of cell free processes could be critical to determining performance bottlenecks, and estimating the costs of cell free manufactured products.

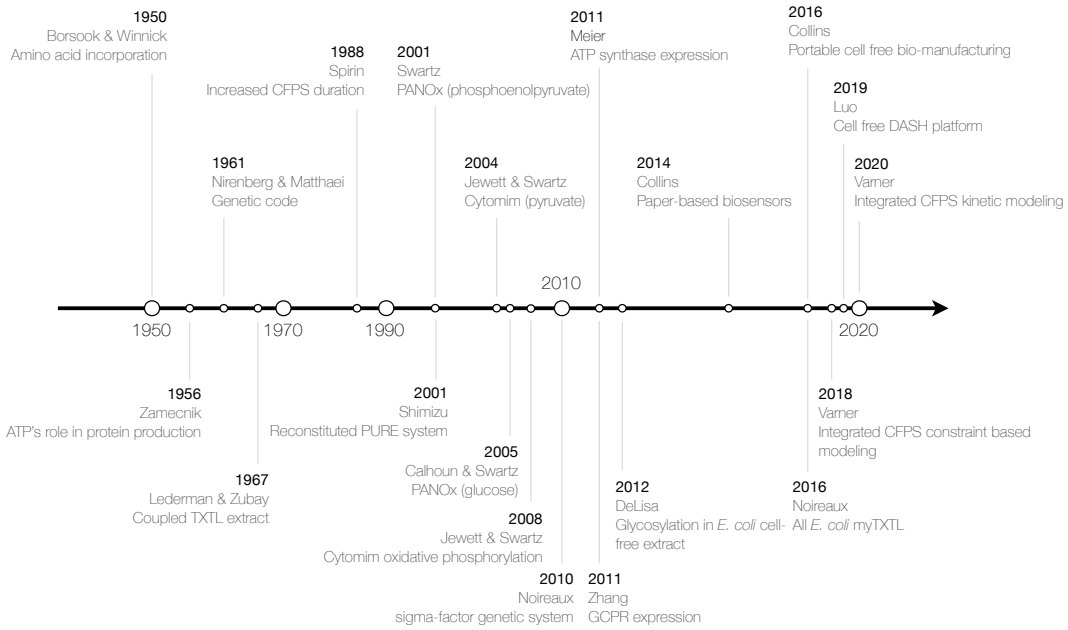

Figure 1.1: Time line for milestones in the evolution of cell free systems since 1950 until now. Abbreviations: cell free protein synthesis (CFPS), G-coupled protein receptor (GCPR), transcription and translation (TXTL).

1.2 Origin and preparation of cell free extracts

There are two broad classes of cell free systems: crude cell lysates and reconstituted systems. While crude extract-based systems, commonly prepared from *E. coli*, *S. cerevisiae*, rabbit reticulocytes, wheat germ and insect cells [139], consist of the biocatalysts remaining after cell lysis, reconstituted systems are well defined, prepared using only the factors essential for protein synthesis: purified enzymes, tRNAs, ribosomes, amino acids and energy molecules. The first purified extract of this kind, the Protein synthesis Using Recombinant Elements (PURE) system, was developed by Shimizu et al. in 2001 [147]. A similar system, based on *Thermus thermophilus*, was later developed by Zhou et al. [197]. Other specialized systems based on PURE have also been developed [76, 124, 112, 51]. These specialized systems have been utilized in applications including the synthesis of disulfide-bonded functional aglycosylated Immunoglobulin G (IgG)

and G-protein coupled receptors, and the study of the effects of liposomes on the solubility of aggregation-prone membrane proteins. Such reconstituted systems offer two main advantages over crude extracts. First, they are a valuable research tool for studying biological processes including protein expression and folding in the context of a completely defined reaction mixture. For example, given the precise knowledge and control of the components in the reconstituted system, it is possible to study the role of individual additions such as chaperones, translation elongation factors, ribosome release factors, and other molecules. Li et al., in a study analyzing the influence of such additions in the PURE system, showed that the efficiency of protein synthesis was limited by translation elongation capacity, ribosome release and ribosome recycling. When the authors changed the ratio of elongation factors, release factors and recycling factors to ribosome concentration to more closely resemble *in vivo* conditions, a 5-fold improvement in the yield of firefly luciferase reporter protein was observed [97]. The second advantage of reconstituted systems, such as the PURE system, is that they do not contain proteases and nucleases, further improving the production of many proteins [163]. Despite these advantages, reconstituted systems suffer from two major drawbacks: higher cost (\$0.99/μL for a PURE reaction vs. \$0.15–0.57/μL for a crude extract reaction; price for commercial kits [55]), and typically lower yields [67]. In this regard, crude cell extracts prevail; they are less expensive, especially for reactions carried out in larger scales [163]. They also offer more complex metabolic capabilities that can be exploited for energy regeneration, extending the duration of protein synthesis. Toward these advantages, the preparation of crude cell free extracts, which has undergone a significant evolution since the early applications in the 1950s and 1960s, is now an area of considerable focus.

Cell free extracts are commonly derived from crude cell extracts, where the cell's transcription and translation machinery is retained while cellular debris and chromosomal DNA are discarded (Fig. 1.2). Cells are typically grown until they reach exponential phase, when they are harvested and lysed commonly using a high pressure homogenizer or a specialized bead mill [152]. Early extracts were prepared by centrifugation of lysates at 30000×g followed by the addition of a mixture of amino acids, adenosine triphosphate (ATP) and other energy molecules, salts, and buffer [199, 135]. In the early 2000s, several changes were made by different research groups to make the extract preparation protocol more efficient including centrifugation at a lower rate (12000×g), the use of shake flask fermentation, and the overexpression of the T7 RNA polymerase in the commercial BL21 (DE3) *E. coli* strain during extract preparation [89, 98, 92]. Alternatives to the high pressure homogenization step, which include the use of bead vortex mixing [152] or lytic enzymes [35], have also been recently explored. It is also possible to delete or overexpress certain genes in the source cell to yield customized cell free extracts. For example, the Swartz group made several gene deletions in *E. coli* A19 cells before harvesting and extract preparation, improving the protein yield in the extract by up to 250% [21, 108]. More recently, a new extract design scheme was implemented by the Jewett lab to combinatorially mix different extracts, each containing a unique overexpressed enzyme, to construct a full biosynthetic pathway [38]. The same group also optimized the extract preparation procedure to better accommodate the use of genetic circuits [154]. These developments show that the extract preparation process can be modified depending on the end goal. However, there are still important unanswered questions in extract preparation. For instance, it still remains to be explored how one can selectively delete enzymes only in cell free

extracts. Continued research in this area could pave the way for minimal extracts highly optimized for a known application.

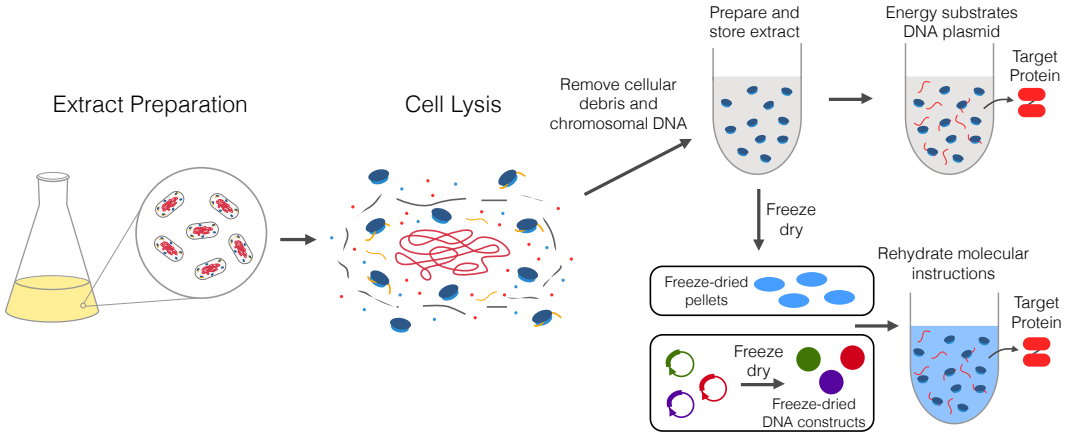

Figure 1.2: Schematic of cell free protein synthesis. Cell extract is prepared by cell lysis and cellular debris and chromosome DNA is removed. An energy source along with necessary amino acids, nucleotides, and cofactor are added to the cell free reaction. Template DNA of the target protein is added. The target protein is then easily purified from the cell free system. Alternatively, cell free extract can be freeze dried into pellets and paired with lyophilized DNA. Through the simple addition of water, proteins can be manufactured on site and on demand. Figure adapted from [23, 132].

1.3 Applications of cell free technologies

1.3.1 Cell free production of biologics and specialized proteins

Cell free protein synthesis (CFPS) has been utilized in a wide range of applications from the production of pharmaceutical proteins [100, 53, 117] to the production of libraries for protein evolution and structural genomics [166]. Complex post-translational modifications that are typically difficult to carry out using bacterial extracts have also recently been achieved in cell free. For example, N-linked glycoproteins have been produced in an *E. coli*-based cell free extract

with the addition of a purified oligosaccharyltransferase (OST) and its lipid-linked oligosaccharides (LLOs) [56]. A single pot glycoprotein synthesis system was also developed, potentially allowing for the production of personalized protein therapeutics [79]; in this system, the OSTs and LLOs were expressed in the *E. coli* host strain which resulted in glycosylation-competent lysates. Other specialized proteins have also been produced in cell free systems. The ability to add membrane mimics such as surfactants or liposomes to the extract as stability agents has allowed the production of membrane proteins [134, 106, 181, 151]. Vaccines [160, 117], protein assemblies [81, 46, 37], and proteins incorporating non-natural amino acids [6, 5, 103] have also been synthesized using CFPS systems. Disulfide-bonded proteins and antibodies have also been synthesized by adding components that facilitate the formation of these bonds to the mixture such as glutathione reductase, thioredoxin reductase, iodoacetamide, and disulfide isomerase (DsbC) [163, 136, 192, 112]. Cytosol-penetrating antibodies have also been synthesized [109]. The cell free synthesis of onconase, a cytotoxic cancer therapeutic, has also been demonstrated [143]. Point-of-care protein manufacturing is also possible when microfluidic reactors are used. Compared to batch reactions, continuous flow microreactors typically offer users more precise control over mixing [64, 107]. An automated on-chip CFPS reactor has been developed that runs transcription and translation reactions simultaneously but in separate compartments [50]. Each process can be optimized independently and the quasi-continuous supply of new mRNA from the TX chamber to the TL chamber allows a longer CFPS reaction and increases protein yield. Other microfluidic platforms integrate purification methods like dialysis and affinity chromatography [118, 113]. For example, cecropin B, an antimicrobial peptide that is widely used to control biofilm-associated diseases, has been produced

at a clinically relevant dose in a few hours using a microfluidic device with on-chip protein purification [113]. A continuous exchange microfluidic reactor using nanofabricated membrane to allow for extended reaction times and improved yields has also been developed with the goal of producing single dose therapeutic proteins at the point-of-care [171]. Moreover, cell free extracts can be lyophilized and stored at -80°C for more than a year without degradation [163]. They can then be rehydrated with water and then incubated using the body's heat to activate the extract components, highlighting the portability and versatility of the cell free platform [153].

Lastly, while the majority of CFPS has been carried out in small scales, there have been continued efforts to scale-up the technology. For example, the scalability of cell free systems has been explored in a few academic studies [180, 164, 193, 127]. Moreover, there are a few examples of industrial-scale cell free protein production for high-value products such as antibodies and cytokines [193, 191], and a few examples of industrial implementations of the technology, most notably by the clinical stage company, Sutro Biopharma and the GreenWorX platform of GreenLight Biosciences. Continued research in the area of scale-up will potentially accelerate industrial adaptation.

1.3.2 Cell free systems in synthetic biology

Applications of cell free systems in synthetic biology are varied, from diagnostics to fundamental discovery and prototyping. Biosensing is an area where cell free systems have recently proven to be useful. They possess a unique advantage over whole cells because of their ability to detect species that are cyto-

toxic or impermeable to the cell wall [153]. These systems have been deployed to detect pathogens such as norovirus [102], Ebola virus [130] and Zika virus [131]. In addition, initial studies have showed that paper-based cell free sensors can detect the presence of heavy metals such as mercury and drugs such as γ-hydroxybutyrate, by utilizing the transcriptional regulators, MerR and BlcR, respectively [54]. The portability offered by these systems further underscores their usefulness in the field. CFPS has also been used in the development of minimal cells, the simplest cellular mimics that consist of only the genes essential for survival. Minimal cells are often described as biological analogs to the hydrogen atom which has served to uncover many fundamental phenomena in chemistry [111]. Their bottom-up construction has been made possible mainly by the advancements in two areas: compartmentalization strategies and programmable genetic circuits [49, 48, 75, 125, 88]. Toward this goal, proteins have been expressed in compartments such as liposomes [133, 48], phospholipid vesicles [150, 125] and hydrogel particles [196], and genetic circuits that encode oscillations [168, 119], negative feedback loops [85], or riboswitches acting as regulatory elements [104] have been developed in CFPS systems. Interacting minimal cells have also been developed [3]. Recently, the construction of dynamic biomaterials powered by artificial metabolism was also demonstrated by Hamada and coworkers, with applications ranging from locomotion, pathogen detection and hybrid nanomaterials [62]. Cell free systems have also been used for prototyping novel genetic parts or circuits before using them *in vivo*. Prototyping can be done more efficiently in cell free systems because of the tighter control over plasmid dosage, inducer concentrations, pH, temperature and salt concentrations [153]. The ability to use linear PCR templates in cell free further accelerates this process [153]. Moreover, developments in experimental setup and analysis

techniques such as the use of acoustic liquid-handling robots [110], real-time fluorescent reporters [120], microfluidics [33], and droplet-based expression [142] have allowed the prototyping to be carried out in high-throughput rates [153]. The relative ease of manipulating cell free systems makes them attractive tools for investigating complex processes.

1.3.3 Cell free metabolic engineering (CFME)

Cell free systems have gained wide interest in metabolic engineering applications, primarily to circumvent the significant barriers of traditional *in vivo* processes [57]. For example, a major challenge in *in vivo* metabolic engineering is achieving high flux through synthetic pathways of interest. This is because cells have their own objectives e.g., growth or maintenance, which drives metabolic flux away from desired pathways. The complexity of living cells also makes computational modeling and optimization of metabolic flux difficult [39]. Cell free systems, on the other hand, can be accurately modeled and the reaction environment tuned according to the bio-synthetic needs. They offer many advantages for the study, manipulation and modeling of metabolism. Central amongst these is direct access to metabolites and the biosynthetic machinery without the interference of a cell wall. This allows interrogation of the chemical microenvironment while the biosynthetic machinery is operating, potentially at a fine time resolution. Eliminating the need to maintain cell viability also allows the full allocation of energy resources to the production of products of interest. Because of these benefits, various metabolic engineering endeavors have been made in both purified and crude cell extracts with promising results.

Several strategies have been implemented in CFME to increase flux through enzymatic pathways and improve product yield. For example, Opgenorth and coworkers [128] designed a molecular purge valve consisting of an NAD^+-dependent reductase enzyme, an $NADP^+$-dependent reductase enzyme, and a NADH-specific oxidase to manage the flux of reducing equivalents. This valve was utilized to produce valuable compounds such as polyhydroxybutyrate bioplastic and prenylated natural products [128, 129, 173]. The authors carried out efficient synthesis of cannabinoids: up to 1.25 g/L and 1.74 g/L of the cannabinoid precursors, cannabigerolic acid and cannabigerovarinic acid, respectively, were synthesized, then converted in a 1-step reaction using cannabidiolic acid synthase, to cannabidiolic acid and cannabidivarinic acid, respectively [173]. The use of co-immobilized enzymes has also been demonstrated *in vitro*, allowing their reuse over more than 7 cycles and highlighting an important step toward large-scale application [28]. In this study, the regulation and identification of inhibitors of the amorpha-4,11-diene (AD) biosynthetic pathway was also carried out, increasing the AD synthesis rate up to 5.7 $\mu mol/L \cdot min$, an approximately 3-fold increase from their previous work (2 $\mu mol/L \cdot min$) [29]. Other important products such as ethanol [59], n-butanol [94], and ethyl(S)-2-ethoxy-3-(p-methoxyphenyl)propanoate (EEHP) [13], along with next generation devices such as an aerobic enzymatic fuel cell from glucose has also been demonstrated [198]. A majority of CFME approaches described thus far have used purified enzymes to form biosynthethic pathways. Recently, Dudley and coworkers implemented a novel technique, combining six crude *E. coli* lysates (each enriched with a unique pathway enzyme) at equal ratios, and one lysate (enriched with three unique pathway enzymes) to construct a complete 20-step enzymatic pathway of limonene synthesis from glucose [40]. This system achieved a pro-

ductivity of 3.8 $mg/L \cdot h$ limonene, just two-fold less than the *in vivo* pathway [8]. In another novel approach, Yi and coworkers [189] used a hybrid system consisting of *E. coli* and cyanobacteria *Synechocystis* sp. PCC6803 cell lysates to demonstrate the synthesis of (R,R)-2,3-butanediol (2,3-BD) from starch, utilizing the presence of starch-degrading enzymes in the cyanobacterial lysate. Thus, cell free technologies have found wide use for the production of high-value small molecule products, at least in the context of research.

Metabolic engineering approaches have also been used to improve cell free protein synthesis. Calhoun and Swartz [19], for example, performed chromsosomal deletions in the source cells to address the problem of cell free amino acid degradation. Gene overexpression approaches have also been used to improve protein yields [184, 16]. CFME has also been used to address certain bottlenecks in CFPS such as the need for energy and cofactor regeneration in cell extracts. One of the early examples involved adding oxalate, CoA and NAD^+ to inhibit a futile cycle while producing ATP from pyruvate [91]. More involved metabolic pathways, including the activation of glycolysis and oxidative phosphorylation, have been utilized in different extracts [82, 19, 20, 80]. These efforts have paved the way for the use of cheaper energy sources (glucose, pyruvate or glutamate) and nucleotides (NMP) as well as increased the duration of the protein synthesis reactions. Similarly, a novel non-oxidative glycolysis pathway has been designed, enabling 100% conservation of carbon in sugar catabolism to acetyl-CoA [14]. However, despite these achievements and the advantages of cell free over *in vivo* processes, a fundamental challenge remains: the optimization of cell free production systems. Due to the complexity and immense interconnectivity of metabolic networks, even for simple prokaryotic organisms like *E. coli*, optimizing network operation toward a desired function is often not intuitive [12].

To this end, the systems-level analyses offered by various mathematical modeling tools, developed for application to *in-vivo* metabolic optimization problems, could prove indispensable for the systematic design of cell free system operation.

1.4 Mathematical modeling of cell free systems

1.4.1 Cell free transcription and translation models

If cell free systems are to become a mainstream technology for advanced applications such as point of care therapeutic manufacturing [132], we must first understand the performance limits of these systems [80]. A critical tool towards this goal is mathematical modeling. There have been several mathematical models of cell free protein synthesis, with the majority of these models exclusively focusing on transcription and translation (TXTL) processes. These models are mostly systems of ordinary differential equations (ODEs) based upon saturation or Hill-like kinetic expressions. As an early example, Karzbrun and coworkers developed a coarse-grained model of transcription and translation for *E. coli* cell free extract [87]. To simplify calculations, this model was based on four enzymes and ten parameters. Transcription and translation processes were assumed to follow Michaelis-Menten kinetics. The authors noted that the protein synthesis rate of their system began to exponentially decay after 1 hour, so their study focused on the first hour of the cell free experiment. This decay was attributed to resource depletion and waste accumulation, an important practical consideration regardless of cell free system used. Stögbauer and coworkers

developed a model that accounts for resource consumption and degradation and identified the bottleneck of protein synthesis [162]. Variables representing transcription and translation resources were added to the model, but the exact identities and quantities of these resources were beyond the scope of the study. The authors attempted to use Hill functions to better predict saturation effects of mRNA and their protein of interest but found that the optimized Hill coefficients were close to one, resulting in Michaelis-Menten-like approximations. Protein yield was determined to be a function of template DNA concentration. This work also found that NTP depletion was not the reason for protein synthesis rate decay; for the specific extract used, ribosome degradation was to blame for rate decay. More recently, Neiß and coworkers published a comprehensive experimentally validated model that identified limiting factors of cell free protein synthesis [121]. An unusual characteristic of this model was the hybrid black box approach: transcription processes were simplified, while the model for translation was detailed. The entire model was a large system of differential algebraic equations (DAEs); a system of eight algebraic equations and over 400 ODEs. Using sensitivity analysis, Neiß found that cell free protein synthesis rates were limited by concentrations of tRNA and elongation factor Tu. A model that captured resource competition in genetic networks was published by Gyorgy and Murry [60]. For a two-protein expression system, simulations that considered both products agreed with experimental data. This model also predicted possible product concentrations in multiple-protein expression systems, and compared different cell free extracts. The authors concluded that resource competition was a key consideration in the design of synthetic gene circuits. The cell free protein synthesis models discussed thus far have been based on experiments in which DNA/protein components were used to construct genetic

networks. However, RNA genetic circuitry has also been explored in the cell free platform, and mathematical models for the system have been developed. Transcriptional regulating RNAs are of interest because they bypass the need for regulatory proteins [101]. In the context of circuit design, regulatory RNAs have been used to create various logic gates and cascades [17, 27]. The first experimentally validated model of a synthetic RNA circuit was published by Hu and coworkers [72]. The model contained 8 ODEs and 13 previously unknown parameters. These parameters were estimated based on results from sensitivity analysis guided experimental design. Taken together, models of transcription, translation, resource competition, and gene regulatory circuits have provided useful information for optimizing cell free biomanufacturing or designing new systems; however, they have each provided an incomplete representation of cell free protein synthesis. CFPS does not just rely on transcription and translation processes, but instead depends upon central carbon metabolism and other metabolic pathways to meet energy and carbon precursor requirements. Thus, more sophisticated models are needed that integrate metabolic pathways with transcription and translation processes. Ultimately, an integrated framework could provide insights into the limitations of CFPS, and generate strategies for improving CFPS performance metrics such as carbon yield, energy efficiency and productivity.

1.4.2 Metabolic modeling frameworks

Traditional approaches to metabolic modeling, which were first developed to describe living cells, could also be applied to cell free systems, thereby addressing an important current limitation. Decades before the genomics revolution,

mechanistically structured *in vivo* metabolic models arose from the desire to predict microbial phenotypes resulting from changes in intracellular or extracellular states [45]. The single cell *E. coli* models of Shuler and coworkers pioneered the construction of large-scale, dynamic metabolic models that incorporated multiple regulated catabolic and anabolic pathways constrained by experimentally determined kinetic parameters [36]. Shuler and coworkers generated many single cell kinetic models, including single cell models of eukaryotes [161, 187], minimal cell architectures [25], and DNA sequence based whole-cell models of *E. coli* [9]. As biological understanding grew, metabolic models became less reductionist and more detailed. Next generation models described cellular processes such as RNA synthesis, chromosome synthesis, regulated catabolic and macromolecular synthesis pathways in detail using ordinary differential equations [172]. For example, Karr et al. (2012) developed a whole cell model of *Mycoplasma genitalium*, accounting for all genes and their interactions in the cell [86]. The model, which was constructed with independent sub-models describing different components of the cell, successfully described the full cellular life cycle at the level of single molecules. However, while undoubtedly important tools, traditional metabolic modeling approaches are often complex, nonlinear and require the estimation of a large number of unknown parameters; a difficult process because of the inherent noisiness of biological data, and the computational burden of repeatedly solving the model equations. To overcome such obstacles, constraint based methods were developed to describe metabolic networks with only a limited need for kinetic parameters [174].

Stoichiometric reconstructions of microbial metabolism, popularized by constraint based approaches such as flux balance analysis (FBA), have become standard tools to interrogate metabolism [96]. FBA and metabolic flux anal-

ysis (MFA) [185], as well as convex network decomposition approaches such as elementary modes [146] and extreme pathways [145], model intracellular metabolism using the biochemical stoichiometry and other constraints such as thermodynamic feasibility [66, 63] under pseudo steady state conditions. Constraint based approaches use linear programming [31] to predict productivity [174, 144], yield [174], mutant behavior [42], and growth phenotypes [126] for biochemical networks of varying complexity, including genome scale networks. Constraint based models have also been used to identify strategies for the overproduction of desired compounds. These strategies include genetic knockouts or the addition of heterologous enzyme pathways to an organism's metabolic network and have been used in developing useful bacterial strains for the production of biofuels [10], high-value chemicals [114, 158, 190] and pharmaceuticals [138, 44]. Stoichiometric reconstructions have been expanded to include the metabolic demands for protein synthesis; Allen and Palsson developed sequence specific constraint based models, based upon the DNA and protein sequences of interest, where transcription and translation processes were integrated with metabolism [7]. Since the early work of Allen and Palsson, sequence specific constraint based models have been expanded to the genome-scale with detailed descriptions of gene expression (ME-Model) [170, 96, 126] and protein structures (GEM-PRO) [195, 26]. These expansions have greatly increased the scope of questions stoichiometric reconstructions can explore. For example, constraint based methods, which are powerful tools to estimate the performance of metabolic networks, could potentially predict nonintuitive strategies to optimize the interaction between metabolism and gene expression in cell free applications. Thus, the use of integrated constraint based models for cell free optimization studies is a promising future research direction.

1.4.3 Emergence of integrated cell free models

Modeling the integration of cell free transcription and translation processes with metabolic pathways remains in its infancy, with only a few published mathematical models [32, 178, 71]. Horvath and coworkers developed an ensemble of dynamic *E. coli* CFPS models using parameters estimated from measurements of metabolite, amino acid, and protein concentrations from CFPS reactions conducted using the PANOx-SP system [71]. This work built upon the hybrid cell free modeling approach of Wayman and colleagues, which integrated kinetic modeling with a rule-based description of allosteric control [183]. By simulating reaction group knockouts, Horvath et al. suggested that cell free metabolism and protein synthesis were strongly coupled with oxidative phosphorylation and glycolytic flux. On the other hand, to circumvent computationally expensive parameter estimation, Vilkhovoy and coworkers [178] developed an experimentally validated constraint-based model of CFPS which integrated the expression of a model protein product with the supply of metabolic precursors and energy (Fig. 1.3). This model coupled transcription and translation processes with available resources using only six adjustable parameters. Model analysis suggested protein expression in the PANOx-SP system was translationally limited. Further, the same modeling approach, using only a limited number of experimentally derived parameters, also described protein expression in the myTXTL system, thereby underscoring the power and versatility of the approach. Taken together, the incorporation of complex metabolism with genetic regulatory networks using constraint based modeling is a promising approach to simulate cell free systems. Unfortunately, despite these early studies, there remains an unmet need for comprehensive metabolic models of cell free reactions. However, as experimental methods are developed for cell free e.g., [176],

and benchmark cell free data sets are published, we expect the metabolic modeling community will address this shortcoming.

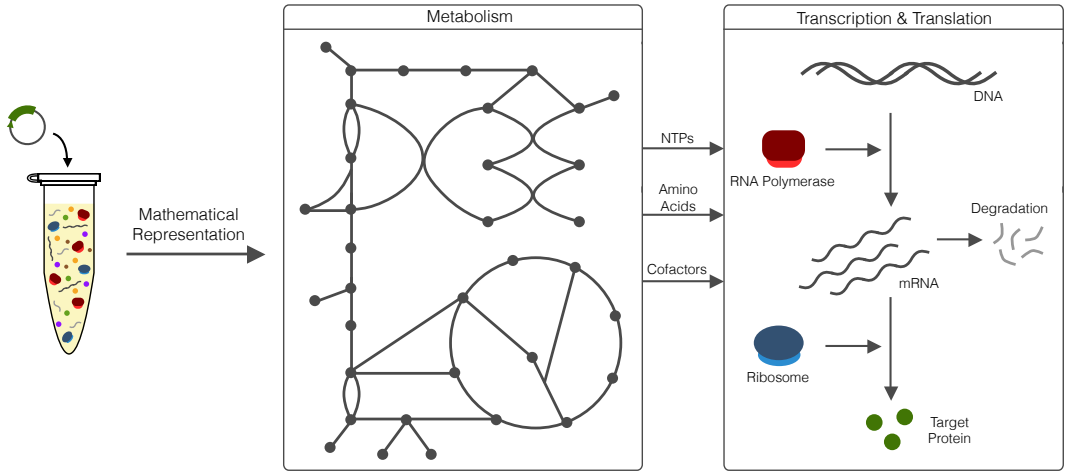

Figure 1.3: Schematic of the integration of transcription and translation processes with metabolism. Transcription and translation processes demand macromolecular precursors (e.g. NTPS, amino acids and cofactors) from metabolism for gene expression. The target protein in turn can affect enzymatic flux (orange arrow) or the target protein is synthesized as a product (green arrow). The integrated framework is represented as a stoichiometric matrix of metabolites participating in certain reactions, where the flux is estimated subject to constraints, a pseudo-steady state assumption and an objective function. Figure adapted with permission from [178].

1.5 Conclusion

Cell free systems have evolved from an investigative tool used since the early 1950s to a sophisticated platform useful for a variety of bioengineering, biomanufacturing, and synthetic biology applications. With the recent advances in extract preparation, improvements in energy regeneration mechanisms, and the ability to perform high throughput continuous reactions in microfluidic chips, cell free systems are emerging as a viable alternative to traditional living cells in several application areas. For example, they have become a valuable investiga-

tive tools for metabolic engineering research, given their tunability and the unfettered access to metabolism without the interference of the cell wall. However, the optimization of cell free applications remains an important challenge. Toward this challenge, mathematical and computational modeling is a critical tool that could move the platform forward. Models facilitate the understanding of the role of systems-level parameters and interactions, and they also promote the generation of metabolic engineering strategies, for example assisting in making the appropriate genetic manipulation for a desired function, which is not always intuitive. The broad review of literature presented here has highlighted several experimental and computational opportunities that could be addressed in future work. For example, a more detailed description of transcription and translation reactions has been utilized in genome scale metabolic engineering models e.g., O'Brien et al [126]. These template reactions could be adapted to a cell free system, allowing us to consider important facets of protein production, such as the role of chaperones in protein folding. In addition, post-translational modifications such as glycosylation that are important for the production of therapeutic proteins could also be included in the next generation of cell free models. Finally, constraint based modeling could be extended to multi-protein synthetic circuits, RNA circuits or small molecule production. There are also opportunities to explore with regard to the preparation and manipulation of cell extracts. For example, enabling selective enzyme deletions directly in cell free extracts, without having these deletions stem from the extract preparation process, could be a game changing technology. Taken together, continual advancements in modeling and experimental design have paved the way for cell free systems to become valuable tools for molecular biology research, and a promising platform for manufacturing of valuable biotherapeutics and chemicals.

However, while the popularity of cell free systems has grown dramatically in the research community, the platform still faces important challenges for biomanufacturing applications, in particular scale-up, the high cost of extracts, and limited post-translational modification capability. While mammalian and insect cell free systems have post-translational modification machinery, these types of extracts are expensive compared to their bacterial counterparts. Toward this challenge, DeLisa and coworkers [56, 79] recently expressed N-linked glycoproteins in *E. coli* cell free extracts, opening up possibilities for the production of therapeutically-relevant proteins in bacterial extracts, which have better overall protein yields, are relatively inexpensive, and have easier extract preparation protocols. There have also been studies on the possible scale-up of protein synthesis by several research groups, and a few startup biotechnology companies. However, this remains a critical and underserved topic area. Another possible challenge to using cell free systems for applications such as biosensors, on-demand therapeutics, or even industrial production, is the inability to achieve 100% lysis of cells during the extract preparation process, resulting in residual contaminating cells. Addressing this concern could be important to meet various Food and Drug Administration (FDA) regulations. Toward this challenge, Smith and coworkers assessed decontamination strategies, and have shown that sterile filtration and lyophilization effectively removes cell contamination without affecting the protein synthesis capabilities of the system [156]. Thus, while there remain important challenges to be overcome, it is encouraging that several research groups have worked toward addressing the challenges faced by the the platform. However, continued research and development is important to further improve the capabilities of cell free technology.

1.6 Acknowledgments

The work described was supported by the Center on the Physics of Cancer Metabolism through Award Number 1U54CA210184-01 from the National Cancer Institute. The content is solely the responsibility of the authors and does not necessarily represent the official views of the National Cancer Institute or the National Institutes of Health.

1.7 Abbreviations

The following abbreviations are used in this manuscript:

CFPS	cell free protein synthesis
TXTL	transcription and translation
DNA	deoxyribonucleic acid
RNA	ribonucleic acid
NMP	nucleoside monophosphate
NTP	nucleoside triphosphate
ATP	adenosine triphosphate
GTP	guanosine triphosphate
NAD	nicotinamide adenine dinucleotide
CoA	coenzyme A
mRNA	messenger RNA
tRNA	transfer RNA
PURE	Protein synthesis Using Recombinant Elements
ODE	ordinary differential equation
CFME	cell free metabolic engineering
FBA	flux balance analysis
MFA	metabolic flux analysis
ME	metabolic engineering
PCR	polymerase chain reaction

CHAPTER 2

ABSOLUTE QUANTIFICATION OF CENTRAL CARBON METABOLITES AND NUCLEOTIDE CHARGED SUGARS BY REVERSED-PHASE LIQUID CHROMATOGRAPHY-MASS SPECTROMETRY

2.1 Abstract

[1] Cell-free protein synthesis (CFPS) is a widely used research tool in systems and synthetic biology; however, if CFPS is to become a mainstream technology for applications such as point-of-care manufacturing, we must understand the performance limits of these systems. Toward this question, we developed a robust protocol to quantify 40 compounds involved in glycolysis, the pentose phosphate pathway, the tricarboxylic acid cycle, energy metabolism and cofactor regeneration in CFPS reactions. The method uses internal standards tagged with 13C-aniline, while compounds in the sample are derivatized with 12C-aniline. The internal standards and sample were mixed and analyzed by reversed-phase liquid chromatography-mass spectrometry (LC/MS). The co-elution of compounds eliminated ion suppression, allowing the accurate quantification of metabolite concentrations over 2-3 orders of magnitude where the average correlation coefficient was 0.988. Five of the forty compounds were untagged with aniline, however they were still detected in the CFPS sample and quantified with a standard curve method. The chromatic run takes approximately 10 minutes to complete. In summary, we developed a fast, robust method to separate, and accurately quantify 40 compounds involved in CFPS

[1] Adapted with permission from Vilkhovoy, M.; Dai, D.; Vadhin, S.; Adhikari, A.; Varner, J. D. Absolute Quantification of Cell-Free Protein Synthesis Metabolism by Reversed-Phase Liquid Chromatography-Mass Spectrometry. JoVE 2019, No. 152, 60329.

in a single LC/MS run. Taken together, the method is a robust and accurate approach to characterize cell free metabolism, so that ultimately, we can understand and improve the yield, productivity and energy efficiency of cell free systems.

2.2 Introduction

Cell-free protein synthesis has become a widely used tool in systems and synthetic biology, and a promising technology for point-of-use manufacturing of biomolecules. Cell-free systems offer many advantages compared to in vivo processes, such as direct access to metabolites and the biosynthetic machinery without the interference of a cell wall or the complications associated with cell growth [69]. However, a fundamental understanding of the performance limits of cell free processes has been lacking. High-throughput methods for metabolite quantification are valuable because they can help characterize metabolism, they are important to our understanding of the systems, and are critical to the construction of robust metabolic computational models useful in process optimization[178, 175, 71]. Common methods used to determine metabolite concentrations include Nuclear Magnetic Resonance (NMR), Fourier transform-infrared spectroscopy (FT-IR), enzyme-based assays, and mass spectrometry (MS)[61, 34, 140, 169]. However, these methods are often limited by their inability to efficiently measure multiple compounds at once and sample size requirements. For example, enzyme-based assays can often only be used to quantify a single compound in a run, and are limited when the sample size is small, such as in cell-free protein synthesis reactions (typically run on a 10-15 μL scale). Meanwhile, NMR requires a high abundance of metabolites for

detection and quantification[34]. Toward these shortcomings, chromatography methods in tandem with mass spectrometry (LC/MS) provide several advantages, including sensitivity and the capability of measuring multiple species simultaneously[41]; however, the analytical complexity increases considerably with the number and diversity of species being measured. It is important, therefore, to develop methods that fully realize the high-throughput potential of LC/MS systems. Compounds in a sample are separated by liquid chromatography and identified through mass spectrometry. The signal of the compound depends on its concentration and ionization efficiency, where the ionization can vary between compounds and may also depend on the sample matrix.

Achieving the same ionization efficiency between the sample and standards is a challenge to using LC/MS to quantify analytes. Further, quantification becomes more challenging with metabolite diversity due to signal splitting and heterogeneity in proton affinity and polarity[74]. Lastly, the co-eluting matrix of the sample can also affect the ionization efficiencies of the compounds. To address these issues, metabolites can be chemically derivatized, increasing the separation resolution, and the sensitivity and detection by the LC/MS system, while simultaneously decreasing signal splitting in some cases[74, 73]. Chemical derivatization works by tagging specific functional groups of metabolites to adjust their physical properties like charge or hydrophobicity to increase ionization efficiency[73]. Various tagging agents can be used to target different functional groups like amines, hydroxyls, phosphates, carboxylic acids, etc. Aniline, one such derivatization agent, targets multiple functional groups at once, and adds a hydrophobic component into hydrophilic molecules, increasing their separation resolution and signal[188]. To address the co-eluting matrix ion suppression effect, Yang and coworkers developed a technique based on

Group Specific Internal Standard Technology (GSIST) labeling where standards are tagged with 13C aniline isotopes and mixed with the sample[188, 77]. The metabolite and corresponding internal standard have the same ionization efficiency since they co-elute, and their intensity ratio can be used to quantify the concentration in the experimental sample.

In this study, we developed a protocol to detect and quantify 40 compounds involved in glycolysis, the pentose phosphate pathway, the tricarboxylic acid cycle, energy metabolism and cofactor regeneration in cell-free protein synthesis reactions. The method is based on the GSIST approach, where we used 12C-aniline and 13C-aniline to tag, detect, and quantify metabolites using reversed-phase LC/MS. The linear range of all compounds spanned 2-3 orders of magnitude with an average correlation coefficient of 0.988. This protocol was adapted to detect and quantify 5 nucleotide sugars and used to determine *in vivo*. In conjunction, we used a commercially available method by Waters to tag, detect and separate all 20 amino acids in the cell-free extract. This method had a linear range for 2 orders of magnitude and an average correlation coefficient of 0.999. Thus, the method is a robust and accurate approach to interrogate cell free metabolism, and possibly whole-cell extracts.

2.3 Results

2.3.1 Aniline tagged metabolites

As a proof-of-concept, we used the protocol to quantify metabolites in myTXTL, a commercially available E. coli based CFPS system (Arbor Biosciences) express-

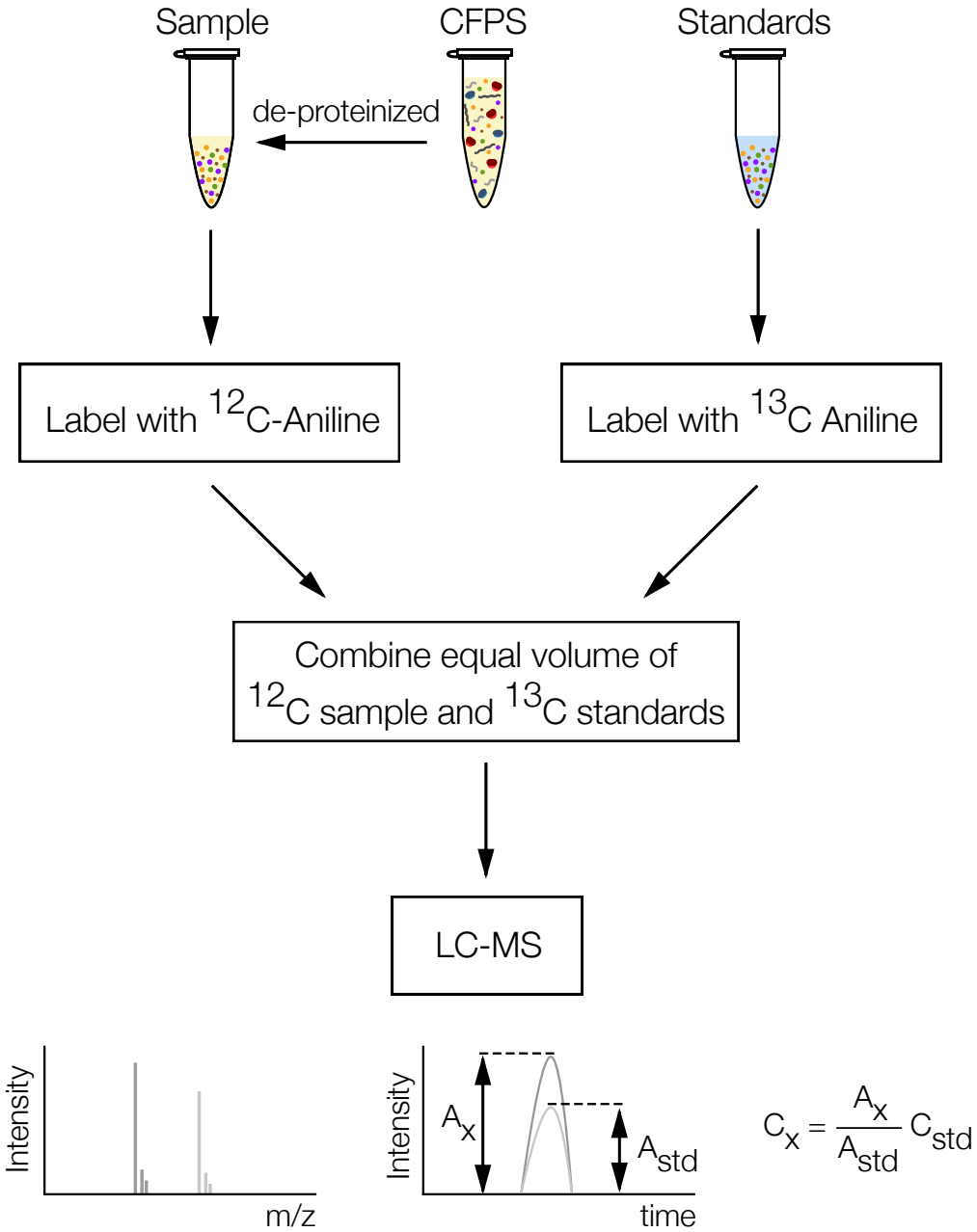

Figure 2.1: Schematic of workflow for aniline tagging. The cell-free protein synthesis reaction is de-proteinized and tagged with 12C-aniline, while a standard stock mixture is tagged with 13C-aniline. Both mixtures are then mixed at a 1:1 volumetric ratio and analyzed by LC/MS.

ing green fluorescent protein (GFP). The CFPS reaction (14μL) was quenched and de-proteinized with ethanol. The CFPS sample was then tagged with 12C-aniline, while standards were tagged with 13C-aniline. The tagged sample and standards were then combined and injected into the LC/MS (Fig. 2.1). The protocol detected and quantified 40 metabolites involved in central carbon and energy metabolism using internal standards, while a standard curve for 5 of the metabolites that were not tagged with aniline was also developed (Fig. 2.2 and Table 2.1). The diverse metabolites involved in these pathways were a class of phosphorylated sugars, phosphocarboxylic acids, carboxylic acids, nucleotides, and cofactors. The derivatization with aniline introduced a hydrophobic moiety into hydrophilic molecules which facilitated more effective separation using reversed-phase chromatography[188]. In addition, the method enabled the separation of structural isomer pairs such as glucose 6-phosphate and fructose 6-phosphate in a single LC/MS run. Each compound's mass over charge (m/z) ratio and retention time were identified prior to the experiment by injecting 1mM of one compound at a time and comparing the mass spectrum to the blank (Table 2.2).

The limit of detection and range of linearity for all compounds was estimated by producing a standard curve that ranged from 0.10 μM to 400 μM (Table 2.1). The average correlation coefficient (R^2) for all compounds was 0.988 and most compounds had a linear range of 3-orders of magnitude. Three compounds had notable saturation effects, especially alpha-ketoglutarate which had a linear range from 0.1 μM to 25 μM. Isocitrate and citrate also had saturation effects above 100 μM.

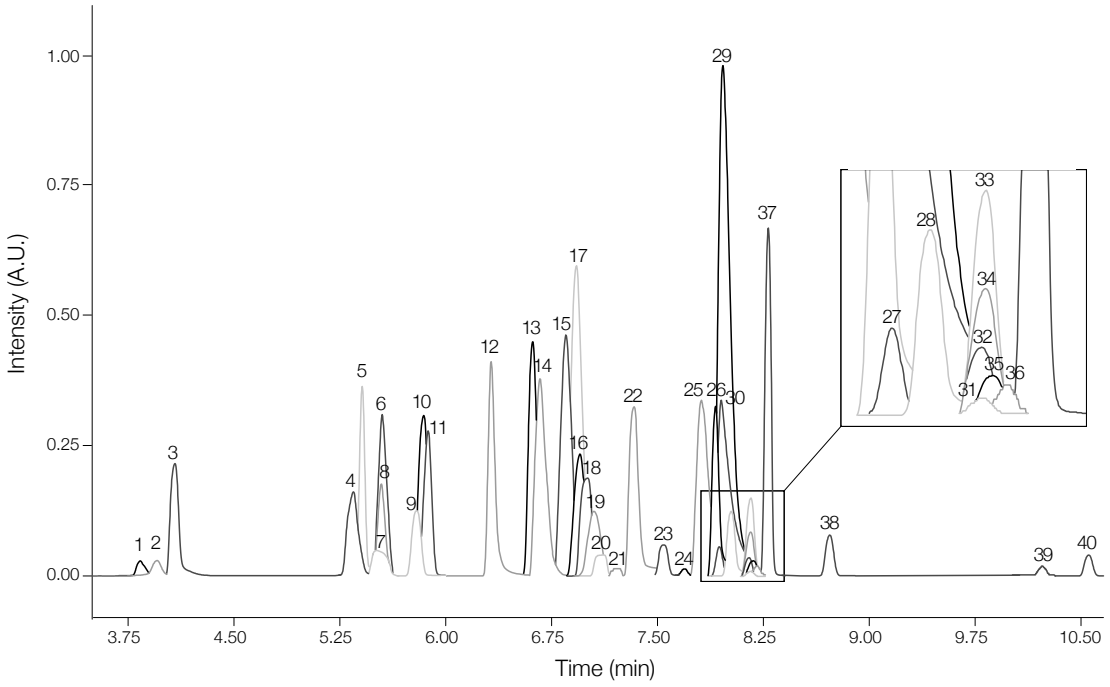

1. Gly3P	9. LAC	17. UDP	25. CTP	33. MAL
2. NAD	10. AMP	18. FAD	26. GTP	34. GAP
3. GLC	11. UMP	19. F16P	27. OAA	35. ACA
4. S7P	12. NADP	20. 6PG	28. aKG	36. NADPH
5. F6P	13. 3PG	21. NADH	29. UTP	37. PEP
6. GMP	14. CDP	22. G6P	30. ATP	38. SUCC
7. RL5P	15. GDP	23. R5P	31. FUM	39. ICIT
8. CMP	16. ADP	24. E4P	32. PYR	40. CIT

Figure 2.2: Mass chromatogram from a single LC/MS run of a 40μM standard mixture of 40 metabolites. Peaks were identified by their retention time and m/z values for each compound. Complete compound names and their abbreviations are listed in Table 2.1.

Table 2.1: Each compound's corresponding limit of detection, range of linearity and correlation coefficient identified from standard curves.

Peak	Metabolite	Abbreviation	KEGG ID	Limit of Detection (μM)	Limit of Linear Range (μM)	R^2
1	Glycerol 3-phosphate	Gly3P	C00093	0.1	400	0.995
2	Nicotinamide adenine dinucleotide	NAD	C00003	0.39	400	0.993
3	Glucose	GLC	C00031	0.1	400	0.997
4	Sedoheptulose 7-phosphate	S7P	C05382	0.16	400	0.988
5	Fructose 6-phosphate	F6P	C00085	0.1	400	0.986
6	Guanosine monophosphate	GMP	C00144	0.39	100	0.992
7	Ribulose 5-phosphate	RL5P	C00199	0.39	400	0.996
8	Cytidine monophosphate	CMP	C00055	0.1	100	0.992
9	Lactate	LAC	C00186	0.1	400	0.988
10	Adenosine monophosphate	AMP	C00020	0.1	100	0.992
11	Uridine monophosphate	UMP	C00105	0.1	100	0.997
12	Nicotinamide adenine dinucleotide phosphate	NADP	C00006	0.34	400	0.950
13	3-Phosphoglyceric acid	3PG	C00197	0.1	100	0.996
14	Cytidine diphosphate	CDP	C00112	0.39	400	0.997
15	Guanosine diphosphate	GDP	C00035	1.5625	400	0.984
16	Adenosine diphosphate	ADP	C00008	0.39	400	0.995
17	Uridine diphosphate	UDP	C00015	0.39	400	0.991
18	Flavin adenine dinucleotide	FAD	C00016	0.1	400	0.958
19	Fructose 1,6-bisphosphate	F16P	C05378	0.39	400	0.989
20	Gluconate 6-phosphate	6PG	C00345	0.39	400	0.989
21	Nicotinamide adenine dinucleotide reduced	NADH	C00004	0.39	100	0.972
22	Glucose 6-phosphate	G6P	C00668	0.1	400	0.984
23	Ribose 5-phosphate	R5P	C00117	0.39	100	0.999
24	Erythrose 4-phosphate	E4P	C00279	0.39	400	0.979
25	Cytidine triphosphate	CTP	C00075	6.25	100	0.998
26	Guanosine triphosphate	GTP	C00044	6.25	100	0.993
27	Oxalacetate	OAA	C00036	0.56	400	0.997
28	Alpha-ketoglutarate	aKG	C00026	0.1	25	0.979
29	Uridine triphosphate	UTP	C00075	1.5625	400	0.998
30	Adenosine triphosphate	ATP	C00002	1.5625	400	0.991
31	Fumarate	FUM	C00122	1.5625	100	0.999
32	Pyruvate	PYR	C00022	0.39	400	0.993
33	Malate	MAL	C00149	0.1	400	0.991
34	D-glyceraldehyde 3-phosphate	GAP	C00118	0.1	100	0.974
35	Acetyl-coenzyme A	ACA	C00024	0.1	100	0.991
36	Nicotinamide adenine dinucleotide phosphate reduced	NADPH	C00005	0.14	100	0.990
37	Phosphoenolpyruvate	PEP	C00074	0.1	100	0.962
38	Succinate	SUCC	C00042	0.1	320	0.999
39	Isocitrate	ICIT	C00311	0.39	100	0.998
40	Citrate	CIT	C00158	0.1	100	0.981

Table 2.2: Each compound's corresponding peak number, retention time, m/z value for 12C, 13C, and unlabeled, cone voltage, and MS species.

Peak	Metabolite	KEGG ID	Retention Time (min)	12C m/z	13C m/z	nonlabel m/z	CV	MS Species
1	Gly3P	C00093	3.85			153	10	M – H2O – H
2	NAD	C00003	3.96			698	10	M + Cl – H
3	GLC	C00031	4.06	289.9	296		15	M + A + Cl - H
4	S7P	C05382	5.41	364	370		10	M + A – H
5	F6P	C00085	5.48	334	340		10	M + A – H
6	GMP	C00144	5.57	437.05	443		10	M + A – H
7	RL5P	C00199	5.58	304	310		10	M + A – H
8	CMP	C00055	5.59	397.09	403		10	M + A – H
9	LAC	C00186	5.77	164.05	170		10	M + A – H
10	AMP	C00020	5.85	421.1	427.1		10	M + A – H
11	UMP	C00105	5.88	398.07	404		10	M + A – H
12	NADP	C00006	6.39			724	10	M - H2O – H
13	3PG	C00197	6.63	242	248.06		15	M + A – H2O – H
14	CDP	C00112	6.72	477	483		10	M + A – H
15	GDP	C00035	6.87	517	523		10	M + A – H
16	ADP	C00008	6.94	501	507		10	M + A – H
17	UDP	C00015	6.97	478	484		10	M + A – H
18	FAD	C00016	7.03			784.15	15	M – H
19	F16P	C05378	7.1	395.95	402.1		10	M + A – H2O – H
20	6PG	C00345	7.11	425.1	437		10	M + 2A – H
21	NADH	C00004	7.23	633.13	639.08		10	M + A + H2O – nicotinamide – H
22	G6P	C00668	7.32	409.1	421.1		10	M + 2A – H
23	R5P	C00117	7.54	379.1	391.1		15	M + 2A – H
24	E4P	C00279	7.71	348.9	361		10	M + 2A – H
25	CTP	C00075	7.84	557	563		5	M + A – H
26	GTP	C00044	7.93	597	603		5	M + A – H
27	OAA	C00036	7.94	281	293		25	M + 2A – H
28	aKG	C00026	7.95	295	307.1		15	M + 2A – H
29	UTP	C00075	7.97	558	564		10	M + A – H
30	ATP	C00002	8.03	581	587		15	M + A – H
31	FUM	C00122	8.09	265	277.1		10	M + 2A – H
32	PYR	C00022	8.09	162	168		25	M + A – H
33	MAL	C00149	8.09	283.06	295.15		10	M + 2A – H
34	GAP	C00118	8.09	319	331.1		5	M + 2A – H
35	ACA	C00024	8.16			790	10	M – H2O – H
36	NADPH	C00005	8.23	694.92	700.82		10	M + A – nicotinamide – H
37	PEP	C00074	8.28	317	329.1		20	M + 2A – H
38	SUCC	C00042	8.64	267.07	279.1		15	M + 2A – H
39	ICIT	C00311	10.13	398	416		10	M + 3A – H2O – H
40	CIT	C00158	10.46	416.1	434.06		20	M + 3A – H

A: represents aniline group under MS Species

2.3.2 Amino Acid Analysis

As a proof-of-concept, we applied a commercially available protocol (Waters Corp.) to quantify amino acids in myTXTL, a commercially available E. coli based CFPS system (Arbor Biosciences) expressing green fluorescent protein (GFP). The CFPS reaction (14μL) was quenched and de-proteinized with ethanol. The de-proteinized sample was then tagged with AccQ-Tag Ultra Derivatization Kit (Waters Corp), separated by reverse-phase liquid chromatography and detected with a TUV at 260nm (Fig. 2.3). The accQ-Tag contained 17 of the 20 amino acids in the amino acid hydrolysate standard. The stock mixture was supplemented with the three missing amino acids: L-glutamine, L-asparagine, and L-tryptophan at the same concentration as the other amino acids. The limit of detection and limit of the linear ranges was determined to range from 0.781 to 50 μM with an average correlation coefficient of 0.999 (Table 2.3). The only exception was L-cysteine which had a linear range of 0.391 to 25 μM with a correlation coefficient of 0.999. L-cysteine had a lower limit of linear range since it's concentration was half of all the other amino acids in the amino acid hydrolysate standard mixture. Amino acids in the sample were identified by their retention time and compared to the standard and quantified by standard curve method.

2.3.3 Nucleotide charged sugars

We developed a protocol for the detection and quantification of five nucleotide charged sugars (Fig. 2.4). Nucleotide charged sugars are important precursors for glycoproteins which are products of interest to be produced in CFPS [79].

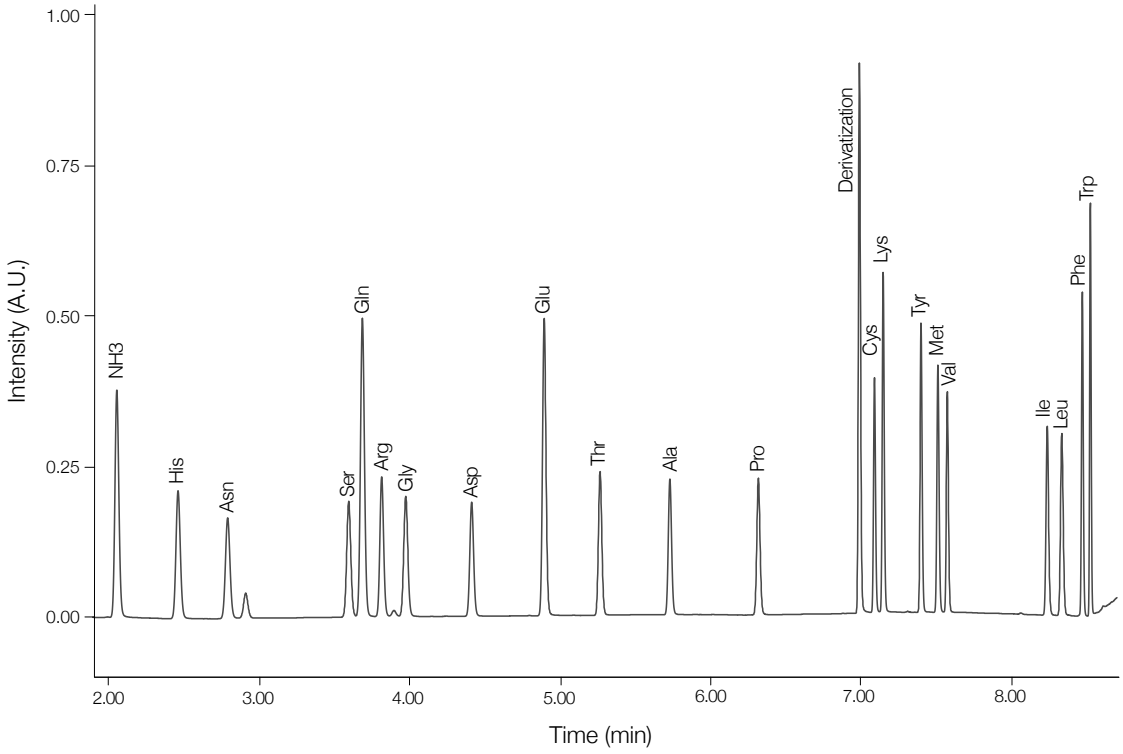

Figure 2.3: Amino acid chromatogram tagged and separated by reverse-phase liquid chromatography and detected with a TUV at 260nm. Peaks were identified by their retention time.

Table 2.3: Each amino acid's retention time separated by reverse-phase liquid chromatography and detected by TUV at 260nm with the corresponding limit of detection, linear range, and correlation coefficient.

Amino Acid	**Abbreviation**	**KEGG ID**	**Retention Time (min)**	**Limit of Detection (μM)**	**Limit of Linear Range (μM)**	**R^2**
L-histidine	His	C00135	2.565	0.781	50	0.999
L-asparagine	Asn	C00152	2.893	0.781	50	0.999
L-serine	Ser	C00065	3.694	0.781	50	0.999
L-glutamine	Gln	C00064	3.788	0.781	50	0.999
L-arginine	Arg	C00062	3.92	0.781	50	0.999
L-glycine	Gly	C00037	4.082	0.781	50	0.999
L-aspartate	Asp	C00049	4.500	0.781	50	0.999
L-glutamate	Glu	C00025	5.009	0.781	50	0.999
L-threonine	Thr	C00188	5.363	0.781	50	0.999
L-alanine	Ala	C00041	5.834	0.781	50	0.999
Lproline	Pro	C00148	6.419	0.781	50	0.999
L-cysteine	Cys	C00097	7.192	0.391	25	0.999
L-lysine	Lys	C00047	7.250	0.781	50	0.999
L-tyrosine	Tyr	C00082	7.501	0.781	50	0.999
L-methionine	Met	C00073	7.611	0.781	50	0.999
L-valine	Val	C00183	7.680	0.781	50	0.999
L-isoleucine	Ile	C00407	8.340	0.781	50	0.999
L-leucine	Leu	C00123	8.438	0.781	50	0.999
L-phenylalanine	Phe	C00079	8.573	0.781	50	0.999
L-tryptophan	Trp	C00078	8.629	0.781	50	0.999

Table 2.4: Each compound's retention time and mass over charge ratio with the corresponding limit of detection, linear range, and correlation coefficient.

Nucleotide Sugar	Abbreviation	Retention Time (min)	m/z	Limit of Detection (μM)	Limit of Linear Range (μM)	R^2
CMP-Sialic Acid	CMP-Neu5AC	1.562	613.10	0.2	20	0.999
GDP-D-Mannose	GDP-D-Man	1.656	604.01	0.2	20	0.999
UDP-a-D-Galactose	UDP-a-D-Gal	1.670	564.96	0.2	20	0.999
UDP-N-acetyl-D-glucosamine/galactosamine	UDP-Hex	1.671	606.00	0.2	20	0.996

The retention time and mass over charge ratio for each compound were determined individually from standards. The range from 0.2 to 20 μM had a linear coefficient of 0.999 for all compounds except UDP-Hex which had a linear coefficient of 0.996 (Table 2.4). Three of the five nucleotide sugars (CMP-Sialic Acid, GDP-D-Mannose, and UDP-a-Galactose) had unique mass over charge ratios that allowed for their detection and quantification. Because UDP-N-acetyl-D-glucosamine and galactosamine had the same retention time of 1.671 minutes and the same m/z of 606.0, they were not distinguishable for individual quantification. Due to this, the compounds were mixed at a 1:1 ratio to be used for quantification in biological samples. This protocol has been used to determine the corresponding concentrations of nucleotide sugars in *E. coli* lysate (Fig. 2.5) [116] and intracellular levels in mammalian cell lines (data not shown).

2.4 Discussion

Cell-free systems have no cell wall, thus there is direct access to metabolites and the biosynthetic machinery without the need for complex sample preparation. However, despite this, very little work has been done to develop thorough and robust protocols to quantitatively interrogate cell-free reaction systems. In this study, we developed a fast, robust method to quantify metabolites in cell-free re-

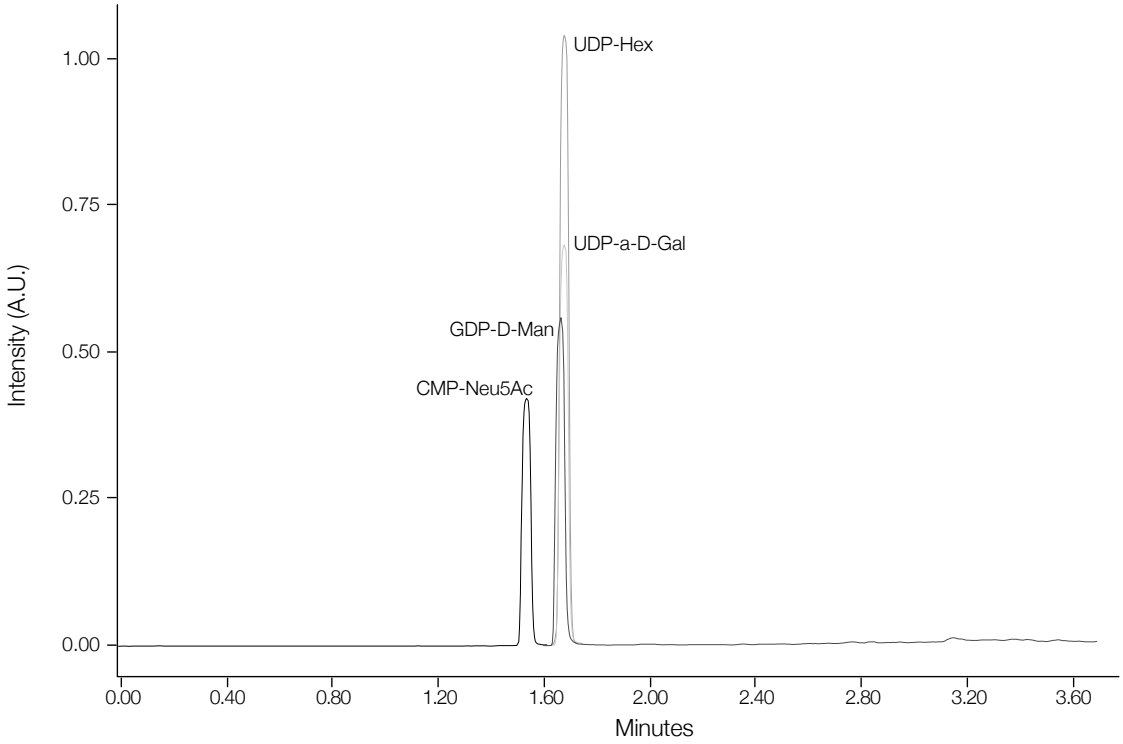

Figure 2.4: Nucleotide charged sugars chromatogram separated by reverse-phase liquid chromatography and detected by mass-spectrometry according to each compounds mass over charge ratio. Peaks were identified by their retention time and selective ion recording.

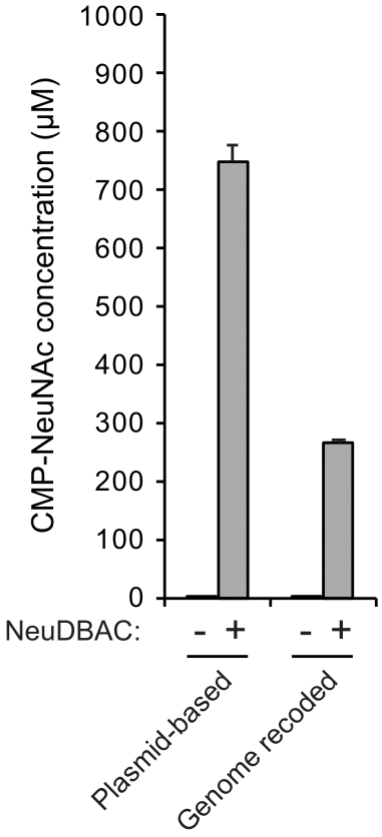

Figure 2.5: Concentrations of *in vivo* sialic acid in glycoengineered *E. coli*, adapted with permission from [116].

action mixtures and potentially in whole-cell extracts. Individual quantification of metabolites in complex mixtures, such as those found in cell-free reactions, or whole-cell extracts, is challenging for several reasons. Central amongst these reasons is chemical diversity. The array of functional groups simultaneously present in these mixtures, such as carboxylic acids, amines, phosphates, hydroxyls, etc. greatly increases the analytical complexity. To circumvent this, we used an aniline derivatization method in combination with 13C internal standard to introduce hydrophobic components to the metabolite mixtures. Using this method, we robustly detected and quantified 40 metabolites in a cell-free reaction in a single LC/MS run. While we demonstrated this technique in a cell-free reaction mixture, it could also likely be applied to whole-cell extracts, thus, potentially allowing the absolute quantification of intracellular metabolites concentrations. The latter application has relevance to a variety of important questions in biotechnology and human health.

The method presented here was based on a previous technique (GSIST) that was applied to whole-cell extracts of the yeast S. cerevisiae[188, 77]. In this study, we expanded upon which compounds could be detected and quantified to include all 12 nucleotides (xMP, xDP, xTP, where x is A, C, G and U). Addition of these compounds could have important biological implications. For example, these nucleotides are heavily involved in transcription and translation processes, which is one of the central processes of interest in CFPS applications, and more generally the compounds are important in a variety of physiological functions. In addition, we were able to detect acetic acid which is an important metabolite when examining overflow metabolism. However, we did not include it in the study because there was a significant reduction of signal in multiple compounds, especially NADH and NADPH, when acetic acid was added

to the standard mixture. Acetic acid had a high limit of detection of 612 μM, thus at these high levels it had a negative effect on the other metabolites' signals. Despite this, acetic acid can still be detected and quantified in samples by creating a standard curve with just acetic acid in the vial. Acetic acid had a m/z value of 134.0, retention time of 5.78 minutes, and a linear range from 612 μM to 5000 μM (R^2 = 0.986) when tagged with 12C-aniline. The remaining metabolites did not alter each other's ion signal and represent a comprehensive mixture to characterize CFPS metabolism.

Taken together, we developed a fast, robust protocol for the characterization and absolute quantification of 40 compounds involved in glycolysis, the pentose phosphate pathway, the tricarboxylic acid cycle, energy metabolism and cofactor regeneration in CFPS reactions. The method relied on internal standards tagged with 13C-aniline, while the sample was tagged with 12C-aniline. The internal standards and sample compounds co-eluted and eliminated ion-suppression effects which enabled accurate quantification of individual metabolites in complex metabolite mixtures. We identified a total of 40 compounds (41, if including acetic acid) that can be detected and quantified in a cell-free reaction mixture; however, the list of metabolites could be further expanded and adjusted towards the particular biochemical process of interest. Thus, the method provides a robust and accurate approach to characterize cell free metabolism, which is potentially critical to improving the yield, productivity and energy efficiency of cell free processes.

2.5 Materials and Methods

2.5.1 Aniline derivatization

Materials and Reagents: All metabolite standards, aniline, N-(3-dimethylaminopropyl)-N'-ethylcarbodiimide hydrochloride (EDC), tributylamine (TBA), triethyamine (TEA), HPLC grade acetonitrile, and HPLC grade water were purchased from Sigma-Aldrich (St. Louis, MO). Sedoheptulose 7-Phosphate was purchased from Carbosynth (Compton, UK). All materials and equipment are listed in Table A.1 in the appendix.

LC-MS: The UPLC-ESI-MS system consisted of a UPLC system (Acquity H-Class, Waters) and an electrospray ionization (ESI) source mass spectrometer (QDA detector, Waters). The system was controlled by Empower 3 software (Waters). The autosampler was set at 10 ° C. Separation were performed on a Acquity BEH C18 Column (1.7 μm, 2.1 mm x 150 mm, Waters). The elution started from 95% mobile phase A (5 mM TBA aqueous solution, adjusted to pH 4.75 with acetic acid) and 5% mobile phase B (5 mM TBA in Acetonitrile), raised to 70% B in 10 minutes, further raised to 100% B in 2 minutes, and then held at 100% B for 3 minutes and returned to initial conditions over 1 minute and held for 9 minutes to re-equilibrate the column. The flow rate was set at 0.3 mL/min with injection volume as 5 μL. The column was preconditioned by pumping the starting mobile phase mixture for 10 minutes, followed by the gradient protocol specified above 3 times prior to any injections. LC-ESI-MS chromatograms were acquired in negative ion mode under the following conditions: capillary voltage of 10 V, dry temperature at 520°C, and an acquisition range of m/z 100-800. Selected ion recordings were specified for each metabolite and are listed in Table

2.2.

Labeling protocol: A solution of 6.0 M 12C-aniline was prepared by combining 550 μL of aniline with 337.5 μL if water and 112.5 μL of 12 M hydrochloric acid and vortexed.A solution of 6.0 M 13C-aniline solution was prepared by combing 250 mg 13C-aniline with 132 μL water and 44 μL of 12 M hydrochloric acid and vortexed. Store aniline solutions at 4 °C for upto 2 months. EDC at 200.0 mg/mL was prepared freshly in HPLC grade water. A 50 μL sample solution with 35 standards was prepared in water at 40 μM. 5 μL of 13C-aniline was added to the sample solution followed by 5 μL of 200 mg/mL EDC. The CFPS sample was de-proteinized by the addition of 100% ice-cold ethanol at a 1:1 volumetric ratio and centrifuged at 12,000 x g for 15 minutes at 4°C. The supernatant was transferred into a new centrifuge tube and 6 μL was used for aniline tagging. The volume was brought upto 50 μL with water and 5 μL of 12C-aniline and 5 μL of 200 mg/mL EDC was added to the reaction. Both sample and standard mixtures were vortexed with gentle shaking at ambient temperature (22 °C) for 2 h. The labeling reaction was stopped by the addition of 1.5 μL of triethylamine. The mixture was centrifuged at 13,500 xg for 3 minutes. The supernatant of the sample and the standard were combined at a 1:1 volumetric ratio into an autosample vial for injection into the LC-MS. The solution mixture was injected at 5 μL and the 12C-aniline m/z tagged values were recorded. The sample was injected again at the same volume and the 13C-aniline mz values were recorded (Table 2.2). The QDa detector is unable to record both the 12C and 13C m/z values at the same time since it cannot handle that amount of data acquisition. Thus, the sample is injected twice to record the sample intensities followed by the standard intensities.

Standard curve preparation: Prepare a series of dilutions in water of the untagged metabolites (NAD, NADP, FAD, acetyl-CoA and glycerol 3-phosphate) ranging from 0.4 to 400 μM with a volume of 50 μL. Add 5 *mu*L of 12-C aniline and 5 μL of 200 mg/ml EDC and vortex at room temperature for 2 hours. Add 1.5 μL of triethylamine and centrifuge at 13,500 x g for 3 minutes. Transfer the standard into an auto-sample vial and inject into the LC-MS. The untagged metabolites follow the same procedure as the sample to replicate the sample matrix in order to maintain a similar ionization efficiency.

Quantification of metabolites: The mass-chromatogram peak for each metabolite is integrated and the area is used to quantify the amount in the sample by the following equation:

$$C_{x,i} = \frac{A_{x,i}}{A_{std,i}} C_{std,i} D \tag{2.1}$$

where $C_{x,i}$ is the concentration of the unknown sample for metabolite i, $A_{x,i}$ is the integrated area of the unknown metabolite i, $A_{std,i}$ is the integrated area of the internal standard of metabolite i, $C_{std,i}$ is the concentration of the internal standard of metabolite i, and D is the dilution factor.

Untagged metabolites are quantified by the standard curve method where the integrated area of a standard is associated with the known concentration. A standard curve is developed for the series of different concentrations and is used to quantify the unknown amounts in the sample.

2.5.2 Amino acid derivatization

Amino Acid labeling protocol: A solution containing a mixture of 20 amino acids is drivatized with a Waters AccQ-Tag Ultra amino acid analysis kit (Waters). The sample is prepared by taking 10 μL of a mixture of 20 amino acids and adding 70 μL of a buffer solution (Waters) followed by 20 μL of a reagent (Waters). The solution is then kept in a water bath at 55 °C for 10 minutes. The solution is then separated by reverse-phase liquid chromatography with a Acquity Amide C18 Column (2.1 mm x 150 mm, Waters) and analyzed with a TUV detector at 260 nm. The gradient protocol is available from Waters Corporation. Amino acid are detected and quantified based on known retention times (Fig. 2.3).

2.5.3 Nucleotide charge sugar detection

Nucleotide charge sugar protocol: Nucleotide charged sugars were purchased from CarboSynth (Newbury, UK). Standards were dissolved in water individually and injected into an UPLC-ESI-MS (Waters) to determine their corresponding retention times and mass over charge ratios (m/z). The UPLC-ESI-MS system consisted of a UPLC system (Acquity H-Class, Waters) and an electrospray ionization (ESI) source mass spectrometer (QDA detector, Waters). The system was controlled by Empower 3 software (Waters). The autosampler was set at 10 ° C. Separation were performed on a Acquity BEH C18 Column (1.7 μm, 2.1 mm x 150 mm, Waters). Separation were performed on a Acquity BEH C18 Column (1.7 μm, 2.1 mm x 50 mm, Waters). The elution started from 95% mobile phase A (5 mM TBA aqueous solution, adjusted to pH 4.75 with acetic acid) and

5% mobile phase B (5 mM TBA in Acetonitrile), raised to 57% B in 2 minutes, further raised to 100% B in 0.5 minutes, and then held at 100% B for 2 minutes and returned to initial conditions over 0.1 minute and held for 4 minutes to re-equilibrate the column. The flow rate was set at 0.6 mL/min with injection volume as 5 μL. The column was preconditioned by pumping the starting mobile phase mixture for 10 minutes, followed by the gradient protocol specified above 2 times prior to any injections. LC-ESI-MS chromatograms were acquired in negative ion mode under the following conditions: capillary voltage of 10 V, dry temperature at 520°C, and an acquisition range of m/z 100-800. Selected ion recordings were specified for each metabolite and are listed in Table 2.4.

Detection and quantification of *in vivo* sialic acid

For detection and quantification of nucleotide sugars, *E. coli* cells of interest were pelleted to an equivalent A_{600} of ~ 30, resuspended in 1 mL ultrapure water and lysed by sonication. Following centrifugation at 30,000 × g, the supernatant was collected and analyzed within 4 h. Cleared *E. coli* lysates were diluted twofold in ultrapure water and injected into an UPLC-ESI-MS system (Waters) for analysis. The protocol developed for nucleotide sugars was followed. Selected ion recordings were specified for CMP-NeuNAc. A standard curve was generated using commercial CMP-NeuNAc (CarboSynth). [2]

[2]Adapted with permission from Natarajan, A.; Jaroentomeechai, T.; Cabrera-Sánchez, M.; Mohammed, J. C.; Cox, E. C.; Young, O.; Shajahan, A.; Vilkhovoy, M.; Vadhin, S.; Varner, J. D.; Azadi, P.; DeLisa, M. P. Engineering Orthogonal Human O- Linked Glycoprotein Biosynthesis in Bacteria. Nature Chemical Biology 2020, 16 (10), 1062–1070. https://doi.org/10.1038/s41589-020-0595-9.

2.6 Acknowledgments

The work described was supported by the Center on the Physics of Cancer Metabolism through Award Number 1U54CA210184-01 from the National Cancer Institute (https://www.cancer.gov/). The content is solely the responsibility of the authors and does not necessarily represent the official views of the National Cancer Institute or the National Institutes of Health. The funders had no role in study design, data collection and analysis, decision to publish, or preparation of the manuscript.

CHAPTER 3

STEP-RESPONSE DETERMINATION AND CELL FREE PROTEIN SYNTHESIS ON A CONTINUOUS FLOW MICROREACTOR

3.1 Abstract

Cell free protein synthesis (CFPS) has been utilized in a wide range of applications from the production of pharmaceutical proteins [100, 53, 117] to the production of libraries for protein evolution and structural genomics [166]. While most applications reported in the literature have been performed as batch reactions, continuous flow microreactors typically offer users more precise control over mixing [64, 107] and more efficient heat and mass transfer [33, 113, 11]. In this work, we investigated the step-response of a commercially available micromixer and used it to run CFPS reactions of enhanced green fluorescent protein (eGFP). We conducted step-response experiments, which consisted of changing the volumetric flow rate roughly instantaneously, and observed a qualitatively CSTR-like response. While the protein yield of the chip was 10% of the batch reactions, this experiment established the possibility of CFPS on this particular set up. Taken together, we have characterized a microfluidic mixer chip and confirmed its ability to support CFPS.

3.2 Introduction

[1] Cell free protein synthesis (CFPS) has been utilized in a wide range of applications from the production of pharmaceutical proteins [100, 53, 117] to the production of libraries for protein evolution and structural genomics [166]. While most applications reported in the literature have been performed as batch reactions, continuous flow microreactors typically offer users more precise control over mixing [64, 107] and more efficient heat and mass transfer [33, 113, 11]. An automated on-chip CFPS reactor has been developed that runs transcription and translation reactions simultaneously but in separate compartments [50]. Other microfluidic platforms integrate purification methods like dialysis and affinity chromatography [118, 113]. A continuous exchange microfluidic reactor using nanofabricated membrane to allow for extended reaction times and improved yields has also been developed with the goal of producing single dose therapeutic proteins at the point-of-care [171]. Point-of-care protein manufacturing, which is especially relevant in remote or low-resource settings, is also possible when microfluidic reactors are used. Cell free extracts can be lyophilized or stored at -80°C for more than a year without degradation [163] and then be rehydrated with water to activate the extract components, highlighting the portability and versatility of the cell free platform [153]. In this work, we investigated the step-response of a commercially available micromixer and used it to run CFPS reactions of enhanced green fluorescent protein (eGFP).

Although our end goal was on-chip CFPS, we began by studying the on-chip performance of a simpler enzyme catalyzed pathway. To establish a calibration

[1] Portions adapted with permission from Vilkhovoy, M.; Adhikari, A.; Vadhin, S.; Varner, J. D. The Evolution of Cell Free Biomanufacturing. Processes 2020, 8 (6), 675. https://doi.org/10.3390/pr8060675.

curve for the fluorescent reporter species resorufin, the fluorometric Amplex Red Glucose/Glucose Oxidase Assay Kit (Invitrogen, San Diego, CA, USA) was run as batch reactions in a 96-well plate according to manufacturer instructions. This protocol was adapted for use on a commercially available 18.7 µL dual-inlet microreactor fabricated from glass (Micronit Microtechnologies, NL). The assay consists of two coupled reactions: the oxidation of glucose to gluconolactone and H_2O_2, which is involved in the oxidation of Amplex Red to fluorescent resorufin (Fig. 3.1). While the geometry of the micromixer chip does not include a circulating region, we were curious to see if it behaved more like a continuous stirred-tank reactor (CSTR) than a plug flow reactor (PFR) (Fig. 3.4). We conducted step-response experiments, which consisted of changing the volumetric flow rate roughly instantaneously, and observed a qualitatively CSTR-like response.

Once we established that a simple enzymatic assay could be run on-chip, we wanted to determine if CFPS was possible on the same chip. Our group has previously used the commercially available CFE myTXTL 2.0 (ArborBiosciences, Ann Arbor, MI, USA) to produce eGFP in batch reactions and gather metabolite, amino acid, mRNA, and protein data for FBA models of metabolism [179]. We ran new reactions on-chip to compare the yield of the chip and batch reactors. Total volumetric flow rate was 4.675 L/h to achieve a residence time of 4h for comparison to 4h batch reactions. This reaction duration was selected as it has previously yielded good results. While the protein yield of the chip was 10% of the batch reactions, this experiment established the possibility of CFPS on this particular set up. Taken together, we have characterized the step-response of a microfluidic mixer chip and confirmed its ability to support CFPS.

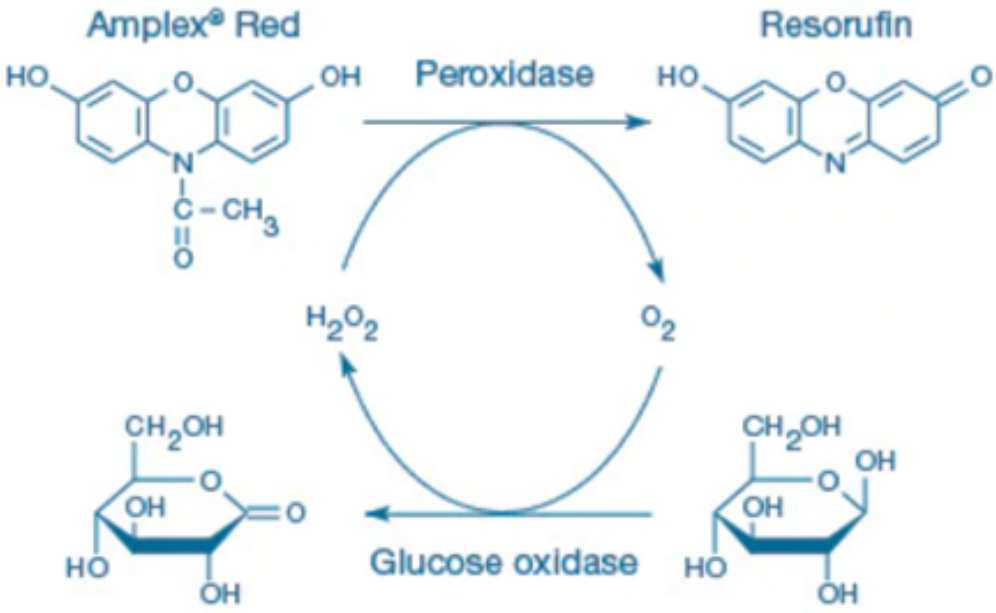

Figure 3.1: Coupled assay reactions catalyzed by glucose oxidase and horseradish peroxidase (HRP), from [1]

3.3 Results

3.3.1 Step-response of microreactor

The resorufin concentration response to flow rate changes was similar to step-up-step-down response in continuous stirred tank reactors (CSTRs) (Fig. 3.2). For each flow rate, relative fluorescence units (RFU) and thus resorufin concentration of collected samples showed oscillatory behavior over several reactor volumes, confirming the reactor was at steady state. For each flow rate change, the resorufin concentration settled within 2τ of the new flow rate. Substrate and reaction mixture (containing enzymes and probe) were infused at equal flow rates by syringe pumps (Fig. 3.4). The initial and step-down total volumetric flow rate was set at 149.6 µL/hr for a residence time of 7.5 minutes. The step-

up total volumetric flow rate was 313.6 µL/hr giving a residence time of 3.0 minutes. Samples were collected every 0.4 reactor volumes.

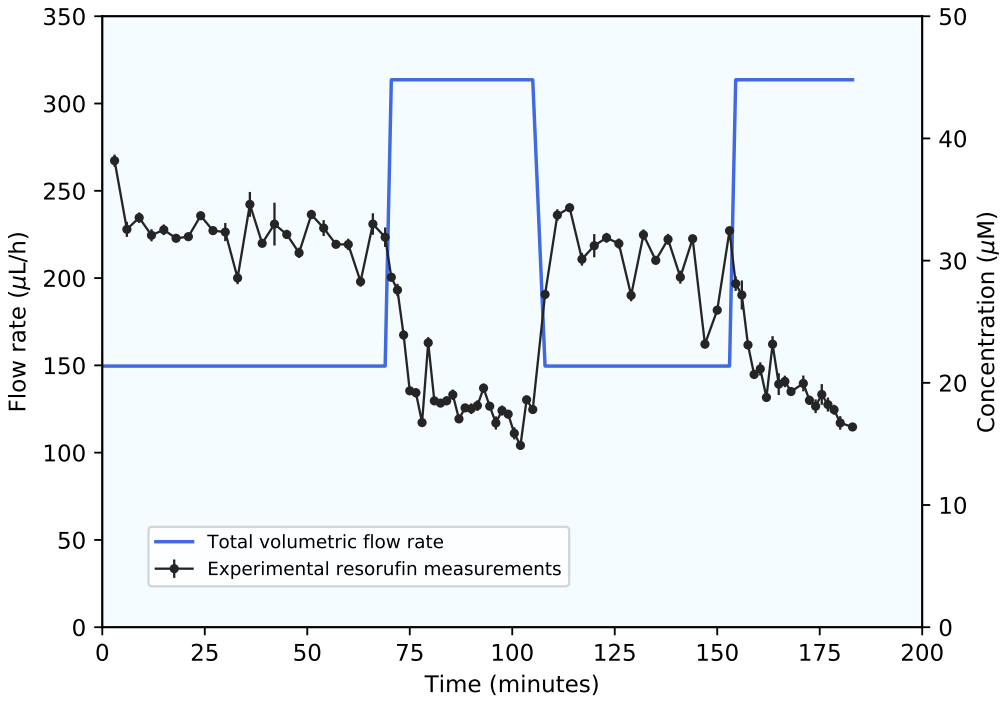

Figure 3.2: Changes in outlet resorufin concentration in response to flow rate changes. Data points represent the mean of three fluorescence readings. Error bars show standard deviation.

3.3.2 On-chip CFPS of enhanced GFP (eGFP)

Although eGFP production was significantly lower than in batch, this experiment demonstrated that we have the capability for on-chip CFPS (Fig. 3.3). For the batch reactions, mean yield was 0.30 ± 0.019 mg/mL, which is on the order of magnitude of the 1.5 mg/mL maximum yield advertised by the manufacturer (ArborBioscience, Ann Arbor, MI). The chip reactions resulted in approximately 10% of the batch yield, with a mean of 0.032 ± 0.0082 mg/mL. At

least three replicates were performed for each reactor condition and residence or incubation times were 4h for all experiments.

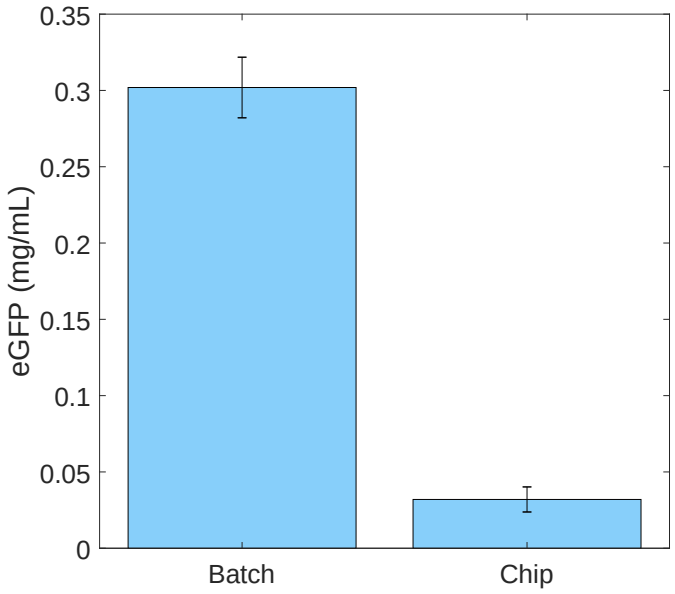

Figure 3.3: GFP yield of batch and chip reactions. Data points represent the mean of three biological replicates. Error bars show standard deviation.

3.4 Discussion

Our data suggest that, while this microreactor has the geometry of a PFR, it may be better represented by a model of n CSTRs. The response curve had a transition period on its way to steady state rather than a time-delayed step change, which is qualitatively more similar to the response of a CSTR than a PFR. While microfluidic systems offer improved heat and mass transfer compared to the macroscale, turbulent mixing does not occur due to small Reynolds numbers [182, 18]. However, serpentine channels such as the one in our micromixer have been used to introduce chaotic advection in aqueous droplets in oil continuous phase [18, 157]. We hypothesize that chaotic advection caused by the serpentine geometry allowed the single phase flow in our study to become well-mixed earlier compared to flow in a straight PFR. Real-time fluorescence monitoring of the reactions may provide some insight into the relationships between degree of mixing, spatial position in the flow channel and time elapsed.

To further investigate our microreactor, we plan to model the system as a set of ordinary differential equations (ODEs) representing a CSTR and compare the simulated results to the experimental results. Parameters will be taken from literature or estimated (as in Table 5.1). The ODEs will be solved for a starting glucose concentration of 100 mM and varying dilution terms. We are interested to see if this microreactor can be modeled as a series of n CSTRs instead of a PFR, which would reduce the model complexity. To write the mass balances for this setup as a CSTR, we assumed that the reaction was well-mixed. Further experiments may contradict this assumption, indicating that a plug flow model is more suitable. With an accurate model, we will be able to optimize the conditions for on-chip CFPS to achieve better yields so that this technology will be a

feasible point-of-care solution.

3.5 Materials and Methods

3.5.1 Step-response of microreactor

A standard curve for the fluorometric Amplex® Red Glucose/Glucose Oxidase Assay Kit (Invitrogen, San Diego, CA, USA) was created based on 100 µL reactions in 96-well plates following kit protocols. This protocol was migrated to a CSTR setup on a commercially available 18.7 µL dual-inlet microreactor fabricated from glass (Micronit Microtechnologies, The Netherlands). Substrate and reaction mixture (containing enzymes and probe) were infused at equal flow rates by syringe pumps (Fig. 3.4). Samples were collected at 0.4-reactor volume intervals and placed on ice to stop the reaction. These were then diluted with assay buffer to a final volume of 100 µL for fluorescence readings at λ_{ex} 560 ± 12 nm, λ_{em} 585 nm on the Varioskan LUX plate reader (Thermo Fisher Scientific, Waltham, MA).

3.5.2 On-chip CFPS of eGFP

For each batch reaction, CFE and plasmid were combined in an Eppendorf tube to create a 12 µL reaction with a plasmid concentration of 5nM. For the chip reaction, plasmid was infused from one syringe pump and CFE from another. Total volumetric flow rate was 4.675 µL/h to achieve a residence time of 4h. This reaction duration was selected as it has previously yielded detectable metabo-

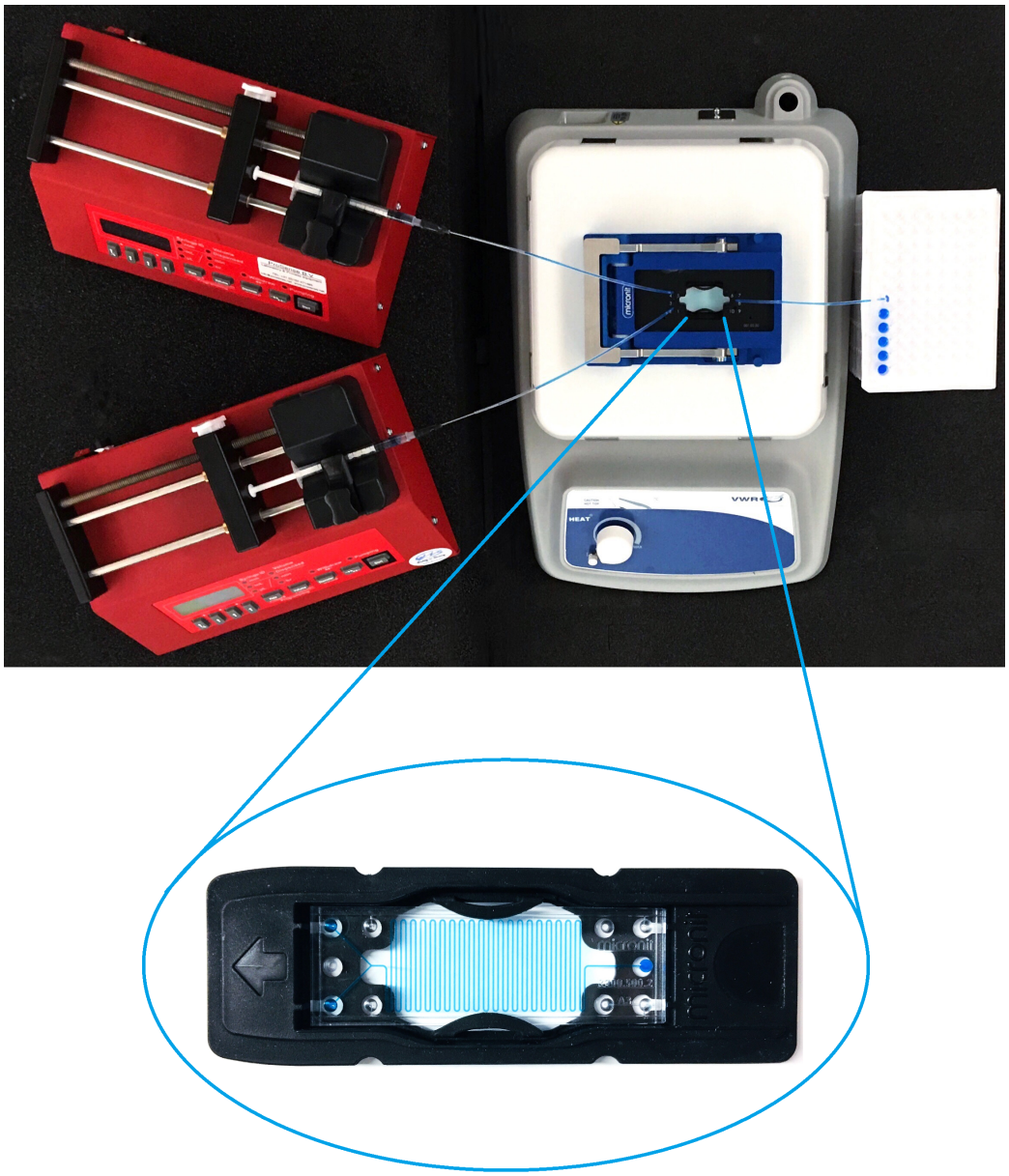

Figure 3.4: Experimental setup. Blue food dye was used to highlight fluid path. Inset: closeup of microreactor chip.

lite, amino acid, mRNA, and protein levels. All CFPS reactions were incubated at 29°C. Metabolites were quantified by LC-MS after aniline derivatization [78]. Amino acid levels were determined using the AccQTag Amino Acid kit (Waters, Milford, MA, USA). Protein levels were detected via fluorescence using a Varioskan Lux (Thermo Fisher Scientific). The eGFP product was quantified ap-

proximately 1 h after completion of CFPS or stored at -80°C and quantified at a later time, well beyond the 8 minute maturation time of eGFP [149]. mRNA levels were measured by RT qPCR using the TaqMan RNA-to-Ct^{TM} 1-Step Kit (Applied Biosystems, Waltham, MA, USA). All CFPS reactions were performed in triplicate, then each replicate was analyzed in triplicate.

CHAPTER 4

CELL FREE PROTEIN SYNTHESIS OF MORPHINE DEHYDROGENASE

4.1 Abstract

Opioids are a class of drugs highly valued for their potent analgesic properties; however, they are also highly addictive and cause severe side effects, including death as a result of respiratory depression. The Centers for Disease Control and Prevention estimate that 130 Americans die daily from opioid overdoses and that the number of opioid overdose deaths in 2017 represents a six-fold increase compared to 1999 [2]. Alternative manufacturing methods may be the disruption needed to overcome the cost and availability issues associated with naloxone, the opioid overdose antidote. Toward this need, we propose the development of a biosynthetic route of naloxone production with morphine as the precursor. In this work, we produced morphine dehydrogenase - an enzyme that catalyzes the oxidation of morphine to morphinone - by cell free protein synthesis (CFPS), taking advantage of the speed of CFPS compared to cell-based culture. Taken together, we have developed a rapid protocol for expression of an enzyme that could serve as the first enzyme in a novel biosynthetic pathway for the production of naloxone.

4.2 Introduction

Opioids are a class of drugs highly valued for their potent analgesic properties; however, they are also highly addictive and cause severe side effects, including

death as a result of respiratory depression. The Centers for Disease Control and Prevention estimate that 130 Americans die daily from opioid overdoses and that the number of opioid overdose deaths in 2017 represents a six-fold increase compared to 1999 [2]. These overdoses include the misuse of both legal and illicit opioids. The opioid antagonist naloxone has been used in the US since 1971 as an overdose antidote [141]. Unfortunately, naloxone's 30 - 60 minute duration of action means that patients often require multiple doses, and the layperson's access may be limited by the high cost of autoinjectors with a two-pack costing over $4000 [2, 58]. Accessible, point-of-care manufacturing may be the disruption needed to overcome the cost and availability issues. Toward this need, we propose the development of a biosynthetic route of naloxone production.

This work introduces the use of biocatalysts as an alternative production method for naloxone, a small molecule μ-opioid receptor (MOR) antagonist. Naloxone is usually semisynthesized from naturally derived opiates, such as morphine, thebaine, or oripavine [43]. There is currently no known fully biosynthetic pathway for naloxone production; however, we have identified enzymes of interest from existing literature. This study focused on morphine dehydrogenase (MDH), a component of a bioluminescent heroin biosensor designed by Rathbone et al.(1996) [137] including heroin esterase from *Rhodococcus sp. H1*, morphine dehydrogenase (MDH) from *P. putida M10*, and luciferase from *V. harveyi* [22, 99]. This biosensor relies on heroin esterase to convert heroin to morphine and MDH to convert morphine into morphinone, with luciferase acting as the reporter [137, 70]. We chose morphine as our starting compound because it is the major degradation product of heroin in the human body [70], allowing us flexibility to adapt this work from a biomanufacturing blueprint to a potential detoxification method (Fig. 4.1). In this work, we turned to cell free protein

synthesis as a platform for rapid expression of our desired enzyme.

Cell free protein synthesis (CFPS) has been used since the mid-20th century to produce proteins without the constraints of living cells. In 1961, Nirenberg and Matthaei used bacterial cell extract to crack the genetic code [123]. CFPS is now commonly used to produce pharmaceutical proteins, develop large protein libraries for protein evolution studies, and produce high-value small molecule products [24]. The platform has advantages over *in vivo* protein production. The lack of a living cell to support allows metabolism to be optimized toward the product of interest [24]. Without a cell membrane or wall, or intracellular compartments, the extract composition can be directly altered and sample acquisition for analysis is simplified. Finally, the use of cell free extract (CFE) allows the bypassing of gene cloning, reducing the duration of the experiment from the order of days to the order of hours. While CFPS has historically suffered from low product yield, short reaction duration, and poor energy substrate cost effectiveness, these metrics have improved since the mid-1990s to make CFPS a feasible method for the production of a variety of proteins and small molecule products [24, 165, 194]. In this work, we used CFPS to produce an enzyme - morphine dehydrogenase - that could serve as the first enzyme in a novel biosynthetic pathway for the production of naloxone from morphine.

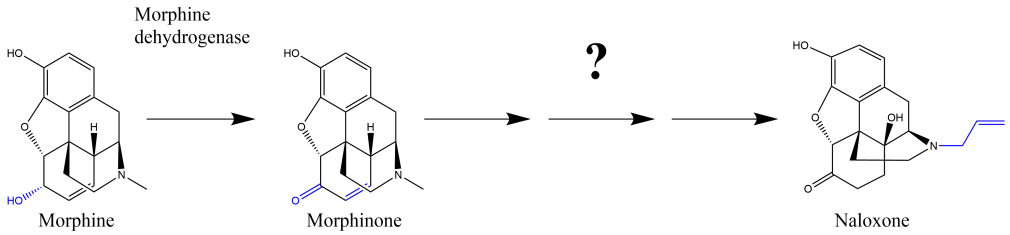

Figure 4.1: Morphine dehydrogenase as the catalyst of the first step in our proposed morphine to naloxone biosynthetic pathway

4.3 Results

While the protein continued to accumulate, mRNA concentrations peaked at 4h of incubation (Figs. 4.2, 4.3). The protein yield at 6h was 0.59 ± 0.003 mg/mL, which is on the order of magnitude suggested by the CFE manufacturer (ArborBioscience, Ann Arbor, MI). The protein product appears pure; there are no contaminating bands on SDS-PAGE gel images (Fig. 4.4). The calculated molecular weights (MW) of the 4h and 6h product were 33.4 kDa and 33.3 kDa, respectively. These are within 0.9% error of our expected MW of 33.1 kDa for 6xHis-tagged MDH. The peak and subsequent decline of mRNA concentration indicate degradation; however, since the protein continued to accumulate, we can assume that protein degradation is not a significant concern at this range of incubation periods.

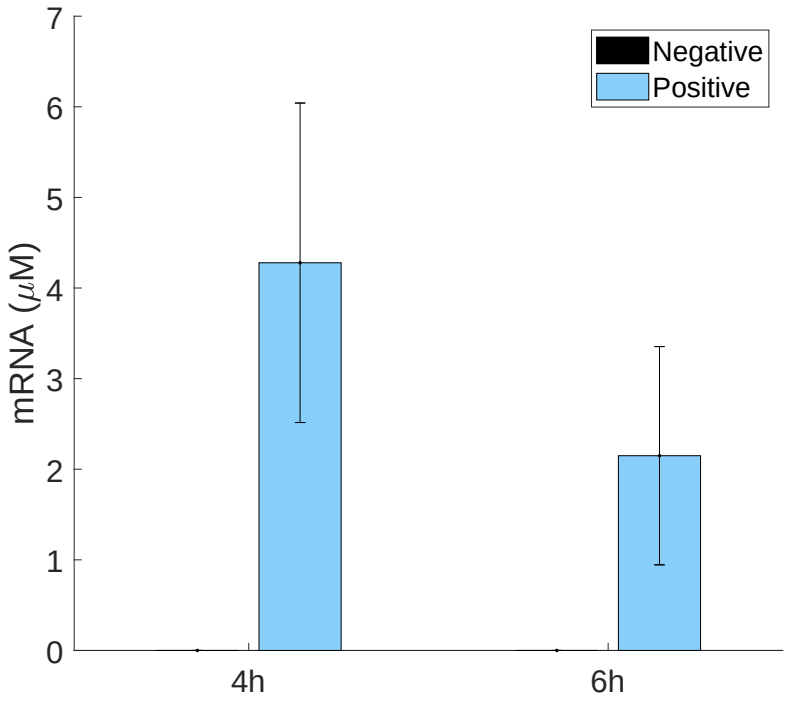

Figure 4.2: mRNA concentration vs. time. Lower mRNA level at 6h indicates degradation. Points represent the mean of three biological replicates and error bars represent the standard deviation.

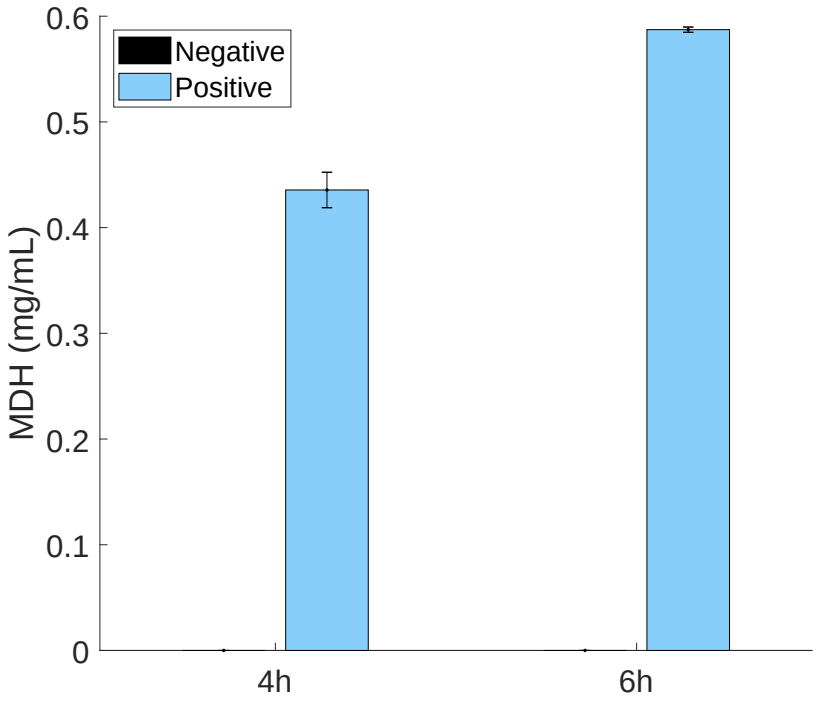

Figure 4.3: Protein yield of CFPS reaction. Values are estimated from analysis of gel images and relative to a standard curve of protein ladder band intensity. Points represent the mean of three biological replicates and error bars represent the standard deviation.

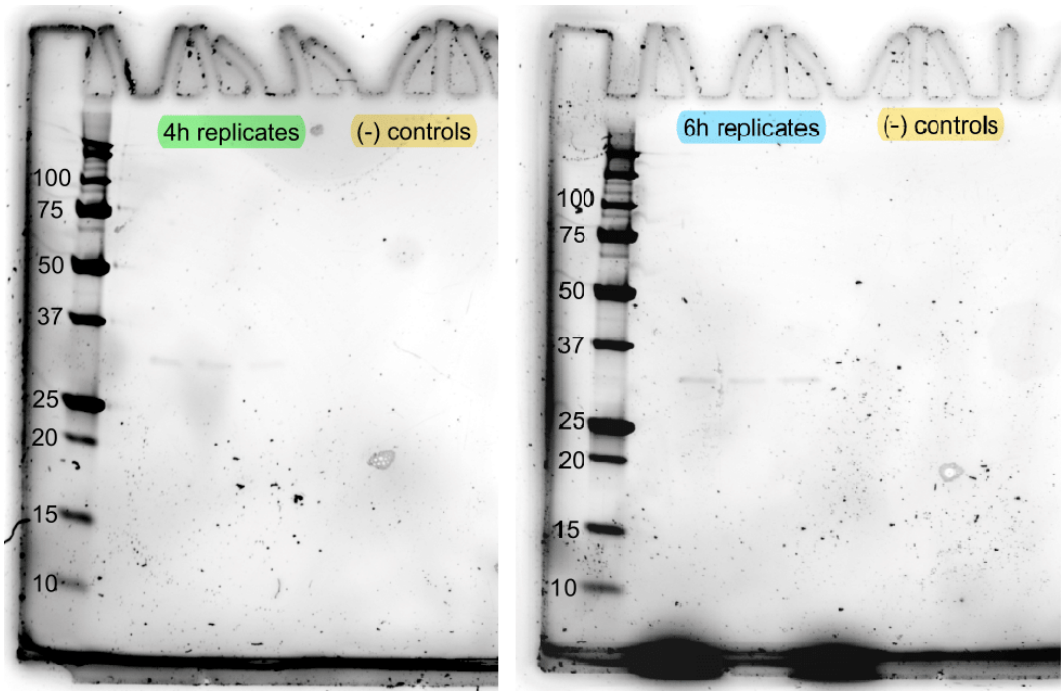

Figure 4.4: SDS-PAGE gels of purified MDH

4.4 Discussion

In this work, we were able to achieve a reasonable yield of MDH from our cell free system within the relatively short production time of 6h. Nonetheless, this study could be improved in a few ways. First, an absolute quantification of protein yield would be preferable to the current relative quantification method. During this study, we discovered that the Qubit Protein Assay (Invitrogen) is not compatible with samples containing imidazole, which interferes with the fluorescence signal measured in the assay. Alternative assays that could be tested include Bradford, BCA, or Lowry protein assays. Determining an absolute concentration of our MDH product would also allow us to determine its catalytic activity by using it in an enzyme activity assay. While it would be ideal to test its activity on morphine, that requires various licenses because it is a Schedule II controlled substance. To determine catalytic activity, the puri-

fied MDH will be substituted for the supplied enzyme in an aldose reductase activity kit, as it is part of that enzyme family. We could also extend incubation times to find an optimal duration that balances product yield and experimental feasibility. Additionally, metabolite values for different time points could be determined and used in metabolic modeling to optimize reaction conditions. Finally, gel resolution could be improved by eluting from the purification column with less buffer to collect a more concentrated protein sample.

4.5 Materials and Methods

4.5.1 Cell Free Protein Synthesis

Cell free protein synthesis (CFPS) reactions of 12 µL volume each were performed in 1.5 mL Eppendorf tubes in triplicate. Linear DNA coding for C-terminally 6xHis-tagged MDH (Twist Bioscience, San Francisco, CA) and NEB-Express GamS Nuclease Inhibitor (New England BioLabs, Ipswich, MA) were added to myTXTL Sigma 70 Master Mix (ArborBiosciences, Ann Arbor, MI). GamS was present in the reaction at 5 µM and linear template at 10 nM. The CFPS reactions were incubated at 29 °C. At least three biological replicates were performed for each time point.

4.5.2 mRNA and Protein Analysis

Following each CFPS run, the total RNA was extracted from 1 µL of the reaction mixture using PureLink RNA Mini Kit (Thermo Fisher Scientific, Waltham,

MA) and stored at -80°C. Gene expression levels were determined by quantitative reverse transcriptase-PCR using AppliedBiosystems™ TaqMan™ RNA-to-CT™ 1-Step Kit (Thermo Fisher Scientific) in combination with custom primers and probe (Integrated DNA Technologies, Coralville, IA). For gene, primer, and probe sequences, see Fig. 4.5 and Table 4.1. An mRNA standard curve was used to determine absolute mRNA concentrations for each of the samples. Three technical qPCR replicates were performed for each biological replicate sample and standard. The mRNA standard was prepared as follows: 15 separate CFPS reactions for 10 nM of linear template were carried out for 4h. Total RNA was extracted using the combined reaction volume. This was followed by the removal of 16S and 23S rRNA using the MICROBExpress™ Bacterial mRNA Enrichment Kit (Life Technologies Corporation). The mRNA standard concentration was determined using the Qubit™ RNA assay kit (ThermoFisher Scientific).

At the end of the CFPS run, 5 µL of each reaction was diluted in 45 µL of Ultrapure water. Protein purification was performed on this diluted mixture using NEBExpress® Ni Spin Columns (New England BioLabs) under native conditions. Eluates were stored at -80 °C until retrieved for quantification. SDS-PAGE on AnyKD Mini Protean TGX Stain-Free Precast Gels (Bio-rad Laboratories, Hercules, CA) was performed to confirm the molecular weight of the expressed protein. Molecular weight calculations were based on standard curves of log MW vs R_f of the ladder proteins (Precision Plus Protein Unstained Standards*, Bio-rad Laboratories). These MW standard curves had R^2 values of at least 0.99. Gel imaging was performed on a ChemiDoc MP (Bio-rad Laboratories). ImageJ (available at https://imagej.nih.gov/ij/) was used to compute the protein yield relative to the amounts in ladder bands by creating linear standard curves of peak area vs. protein amount. Standard curves had R^2 values of

at least 0.99.

Table 4.1: Sequences of primers and probe used in qPCR assay of MDH gene expression, where 6-FAM is the 5′ fluorophore, Iowa Black® FW (3IABkFQ) is the 3′ quencher, and ZEN™ is the internal quencher

Forward primer	5′-TCA ACT GCG ACT ATG GTT ACG-3′
Reverse primer	5′-GAT CGT GGC GTT CCA ATC T-3′
Probe	5′-/56-FAM/ATT TGT ATC /ZEN/ TGC TGC ACT GGC CGA /3IABkFQ/-3′

Figure 4.5: Annotated sequence for C-terminal 6xHis-tagged morphine dehydrogenase. OR2OR1 serves as the promoter for σ70 transcription factor.

CHAPTER 5

CONCLUSION AND FUTURE DIRECTIONS

In this work, we developed a rigorous chromatographic method for the absolute quantitation of central carbon metabolites and nucleotide sugars. This method has been applied to metabolomic and glycosylation studies [177, 116]. We have also begun the modeling of a microfluidic reactor to optimize the process for on-chip, point-of-care manufacturing by cell free protein synthesis. Finally, we have expressed and purified the first enzyme of our proposed novel naloxone biosynthesis pathway. Taken together, we have laid the groundwork for a point-of-care biomanufacturing system for the opioid overdose antidote naloxone.

5.0.1 Future Directions

Modeling of the microreactor

To further investigate our microreactor, we plan to model the system as the following set of ordinary differential equations (ODEs):

$$\frac{d\hat{x}_i}{d\tau} = \sum_{j=1}^{S} v_j \hat{D}_j \hat{x}_{ij} + \sum_{r=1}^{R} \sigma_{ir} \hat{r}_r \tag{5.1}$$

where $\hat{x}_i$ is the dimensionless concentration of species i obtained by dividing the concentration by a characteristic enzyme concentration, τ is dimensionless time obtained by multiplying time by a characteristic rate constant k, S represents the number of streams, v_j is a direction parameter, $\hat{D}_j$ is the dimensionless dilution rate of stream j obtained by dividing the dilution term by k, R is the number of reactions, σ_{ir} is the stoichiometric coefficient of species i for reaction r, and

Enzyme	Substrate	Parameters	References
Glucose oxidase	β-D-glucose	k_{cat} = 297.05 s^{-1} K_M = 18.4 mM	[93, 115, 155] [93, 115, 155, 65, 167, 84]
Horseradish peroxidase	Amplex Red+H_2O_2	k_{cat} = 240 s^{-1} K_M = 0.081 mM	[52] [52]

Table 5.1: Kinetic parameters for Amplex Red glucose assay. Values for glucose oxidase are medians of references cited.

$\hat{r}_r$ is the dimensionless reaction rate obtained by dividing $k_r E_r f(\hat{x})$ by kE. $f(\hat{x})$ is the saturation expression from Michaelis Menten kinetics. Parameters will be taken from literature or estimated (as in Table 5.1). The ODEs will be solved for a starting glucose concentration of 100 mM and varying dilution terms. We are interested to see if this microreactor can be modeled as a series of n CSTRs instead of a PFR, which would reduce the model complexity. To write the mass balances for this setup as a CSTR, we assumed that the reaction was well-mixed. Further experiments may contradict this assumption, indicating that a plug flow model is more suitable. With either resultant model, we will be able to optimize the conditions for on-chip CFPS to achieve better yields so that this technology will be a feasible point-of-care solution.

Further studies of naloxone pathway enzymes and pathway prediction

In this work, we were able to achieve a reasonable yield of MDH from our cell free system within the relatively short production time of 6h. Nonetheless, this study could be improved in a few ways. First, an absolute quantification of protein yield would be preferable to the current relative quantification method. During this study, we discovered that the Qubit Protein Assay (Invitrogen) is not compatible with samples containing imidazole, which interferes with the

fluorescence signal measured in the assay. Alternative assays that could be tested include Bradford, BCA, or Lowry protein assays. Determining an absolute concentration of our MDH product would also allow us to determine its catalytic activity by using it in an enzyme activity assay. While it would be ideal to test its activity on morphine, that requires various licenses because it is a Schedule II controlled substance. To determine catalytic activity, the purified MDH will be substituted for the supplied enzyme in an aldose reductase activity kit, as it is part of that enzyme family. We could also extend incubation times to find an optimal duration that balances product yield and experimental feasibility. Additionally, metabolite values for different time points could be determined and used in metabolic modeling to optimize reaction conditions. Finally, gel resolution could be improved by eluting from the purification column with less buffer to collect a more concentrated protein sample.

Since our ultimate goal is a full pathway from morphine to naloxone, we plan to adapt this method to other enzymes as we predict our pathway. Pathway planning will involve both retrosynthetic analysis and computer aided route planning, where applicable. We are currently developing a deep learning model for single step prediction of metabolic pathways. We hope to extend this work to make multi-step pathway predictions and to identify which enzymes are responsible for the reaction by using prior knowledge of existing alternative paths.[1]

[1] Adapted with permission from Wani, A. A.; Zhang, Z.; Vadhin, S.; Dammalapati, S.; Varner, J. D. Computer Aided Retrosynthesis of Metabolic Pathways. In preparation.

APPENDIX A

SUPPLEMENTAL INFORMATION

Table A.1: List of materials and equipment used to quantify cell-free protein synthesis metabolites with aniline tagging and internal standards

Material/Equipment	Company	Catalog Number	Comments/Description
12C Aniline	Sigma-Aldrich	242284	Aniline 12C
13C labeled aniline	Sigma-Aldrich	485797	Aniline 13C6
3-Phosphoglyceric acid	Sigma-Aldrich	P8877	3PG
Acetic Acid	FisherScientific	AC222140010	ACE
Acetonitrile, LCMS	JT BAKER	9829-03	ACN
Acetyl-coenzyme A	Sigma-Aldrich	A2056	ACA
Acquity UPLC BEH C18 1.7 μM, 2.1 x 150 mm Column	Waters	186002353	Column
Adenosine diphosphate	Sigma-Aldrich	A2754	ADP
Adenosine monophosphate	Sigma-Aldrich	A1752	AMP
Adenosine triphosphate	Sigma-Aldrich	A2383	ATP
Alpha-ketoglutarate	Sigma-Aldrich	K1128	aKG
Citrate	Sigma-Aldrich	251275	CIT
Cytidine diphosphate	Sigma-Aldrich	C9755	CDP
Cytidine monophosphate	Sigma-Aldrich	C1006	CMP
Cytidine triphosphate	Sigma-Aldrich	C9274	CTP
D-glyceraldehyde 3-phosphate	Sigma-Aldrich	39705	GAP
Erythrose 4-phosphate	Sigma-Aldrich	E0377	E4P
Ethanol	Sigma-Aldrich	EX0276	EtOH
Fisher Scientific accuSpin Micro 17 Centrifuge	FisherScientific		Centrifuge
Flavin adenine dinucleotide	Sigma-Aldrich	F6625	FAD
Fructose 1,6-bisphosphate	Sigma-Aldrich	F6803	F16P
Fructose 6-phosphate	Sigma-Aldrich	F3627	F6P
Fumarate	Sigma-Aldrich	F8509	FUM
Gluconate 6-phosphate	Sigma-Aldrich	P7877	6PG
Glucose	Sigma-Aldrich	G8270	GLC
Glucose 6-phosphate	Sigma-Aldrich	G7879	G6P
Glycerol 3-phosphate	Sigma-Aldrich	G7886	Gly3P
Guanosine diphosphate	Sigma-Aldrich	G7127	GDP
Guanosine monophosphate	Sigma-Aldrich	G8377	GMP
Guanosine triphosphate	Sigma-Aldrich	G8877	GTP
Hydrochloric acid	Sigma-Aldrich	258148	HCl
Isocitrate	Sigma-Aldrich	I1252	ICIT
Lactate	Sigma-Aldrich	L1750	LAC
Malate	Sigma-Aldrich	02288	MAL
myTXTL - Sigma 70 Master Mix Kit	ArborBiosciences	507024	Cell-free protein synthesis
N-(3-dimethylaminopropyl)-N'-ethylcarbodiimide hydrochloride	Sigma-Aldrich	03449	EDC
Nicotinamide adenine dinucleotide	Sigma-Aldrich	43410	NAD
Nicotinamide adenine dinucleotide phosphate	Sigma-Aldrich	N5755	NADP
Nicotinamide adenine dinucleotide phosphate reduced	Sigma-Aldrich	481973	NADPH
Nicotinamide adenine dinucleotide reduced	Sigma-Aldrich	N8129	NADH
Oxalacetate	Sigma-Aldrich	O4126	OAA
Phosphoenolpyruvate	Sigma-Aldrich	P0564	PEP
Pyruvate	Sigma-Aldrich	P5280	PYR
Ribose 5-phosphate	Sigma-Aldrich	R7750	R5P
Ribulose 5-phosphate	CarboSynth	MR45852	RL5P
Sedoheptulose 7-phosphate	CarboSynth	MS07457	S7P
Succinate	Sigma-Aldrich	S3674	SUCC
Tributylamine	Sigma-Aldrich	90780	TBA
Triethylamine	FisherScientific	O4884	TEA
ultrapure water	FisherScientific	10977-015	water
Uridine diphosphate	Sigma-Aldrich	U4125	UDP
Uridine monophosphate	Sigma-Aldrich	U6375	UMP
Uridine triphosphate	Sigma-Aldrich	U6625	UTP
VWR Heavy Duty Vortex	VWR		Vortex
Water, LCMS	JT BAKER	9831-03	WATER
Waters Acquity H UPLC Class Quaternary Solvent Manager	Waters		LCMS
Waters Acquity H UPLC Class Sample Manager FTN	Waters		LCMS
Waters Acquity Qda detector	Waters		LCMS
Waters Empower 3	Waters		Software
Waters LCMS Total Recovery Vial	Waters	186000384c	LCMS Vial

BIBLIOGRAPHY

[1] Amplex® Red Enzyme Assays - US.

[2] Understanding the Epidemic | Drug Overdose | CDC Injury Center, December 2018.

[3] Katarzyna P Adamala, Daniel A Martin-Alarcon, Katriona R Guthrie-Honea, and Edward S Boyden. Engineering genetic circuit interactions within and between synthetic minimal cells. *Nature chemistry*, 9(5):431, 2017.

[4] Cem Albayrak, KC Jones, and James R Swartz. Broadening horizons and teaching basic biology through cell-free synthesis of green fluorescent protein in a high school laboratory course. *Journal of Science Education and Technology*, 22(6):963–973, 2013.

[5] Cem Albayrak and James R Swartz. Cell-free co-production of an orthogonal transfer rna activates efficient site-specific non-natural amino acid incorporation. *Nucleic acids research*, 41(11):5949–5963, 2013.

[6] Cem Albayrak and James R Swartz. Direct polymerization of proteins. *ACS synthetic biology*, 3(6):353–362, 2013.

[7] Timothy E Allen and Bernhard Ø Palsson. Sequence-based analysis of metabolic demands for protein synthesis in prokaryotes. *J Theor Biol*, 220(1):1–18, Jan 2003.

[8] Jorge Alonso-Gutierrez, Eun-Mi Kim, Tanveer S Batth, Nathan Cho, Qijun Hu, Leanne Jade G Chan, Christopher J Petzold, Nathan J Hillson, Paul D Adams, Jay D Keasling, Hector Garcia Martin, and Taek Soon Lee. Principal component analysis of proteomics (PCAP) as a tool to direct metabolic engineering. *Metabolic Engineering*, 28:123–133, 2015.

[9] J C Atlas, E V Nikolaev, S T Browning, and M L Shuler. Incorporating genome-wide dna sequence information into a dynamic whole-cell model of Escherichia coli: application to dna replication. *IET Syst Biol*, 2(5):369–82, Sep 2008.

[10] Shota Atsumi, Taizo Hanai, and James C Liao. Non-fermentative pathways for synthesis of branched-chain higher alcohols as biofuels. *Nature*, 451(7174):86–9, Jan 2008.

[11] Mohammad H. Ayoubi-Joshaghani, Hassan Dianat-Moghadam, Khaled Seidi, Ali Jahanban-Esfahalan, Peyman Zare, and Rana Jahanban-Esfahlan. Cell-free protein synthesis: The transition from batch reactions to minimal cells and microfluidic devices. *Biotechnology and Bioengineering*, 117(4):1204–1229, 2020. _eprint: https://onlinelibrary.wiley.com/doi/pdf/10.1002/bit.27248.

[12] JE Bailey. Toward a science of metabolic engineering. *Science*, 252(5013):1668–1675, 1991.

[13] Matthias Bechtold, Elisabetta Brenna, Christian Femmer, Francesco G Gatti, Sven Panke, Fabio Parmeggiani, and Alessandro Sacchetti. Biotechnological development of a practical synthesis of ethyl (s)-2-ethoxy-3-(p-methoxyphenyl) propanoate (eehp): over 100-fold productivity increase from yeast whole cells to recombinant isolated enzymes. *Organic Process Research & Development*, 16(2):269–276, 2011.

[14] Igor W Bogorad, Tzu-Shyang Lin, and James C Liao. Synthetic non-oxidative glycolysis enables complete carbon conservation. *Nature*, 502(7473):693, 2013.

[15] Henry Borsook. Protein turnover and incorporation of labeled amino acids into tissue proteins in vivo and in vitro. *Physiological Reviews*, 30(2):206–219, 1950.

[16] Marcus E Boyer, James A Stapleton, Jon M Kuchenreuther, Chia-wei Wang, and James R Swartz. Cell-free synthesis and maturation of [fefe] hydrogenases. *Biotechnol Bioeng*, 99(1):59–67, 2008.

[17] Sabine Brantl and E. Gerhart H. Wagner. Antisense RNA-mediated transcriptional attenuation: an in vitro study of plasmid pT181. *Molecular Microbiology*, 35(6):1469–1482, 2000.

[18] Michelle R. Bringer, Cory J. Gerdts, Helen Song, Joshua D. Tice, and Rustem F. Ismagilov. Microfluidic systems for chemical kinetics that rely on chaotic mixing in droplets. *Philosophical transactions. Series A, Mathematical, physical, and engineering sciences*, 362(1818):1087–1104, May 2004.

[19] Kara A. Calhoun and James R. Swartz. An Economical Method for Cell-Free Protein Synthesis using Glucose and Nucleoside Monophosphates. *Biotechnol Prog*, 21(4):1146–53, 2005.

[20] Kara A Calhoun and James R Swartz. Energizing cell-free protein synthesis with glucose metabolism. *Biotechnol Bioeng*, 90(5):606–13, Jun 2005.

[21] Kara A Calhoun and James R Swartz. Total amino acid stabilization during cell-free protein synthesis reactions. *Journal of biotechnology*, 123(2):193–203, 2006.

[22] G W Cameron, K N Jordan, P J Holt, P B Baker, C R Lowe, and N C Bruce. Identification of a heroin esterase in Rhodococcus sp. strain H1. *Applied and Environmental Microbiology*, 60(10):3881–3883, October 1994.

[23] Erik D Carlson, Rui Gan, C Eric Hodgman, and Michael C Jewett. Cell-free protein synthesis: applications come of age. *Biotechnol Adv*, 30(5):1185–94, 2012.

[24] Erik D. Carlson, Rui Gan, C. Eric Hodgman, and Michael C. Jewett. Cell-Free Protein Synthesis: Applications Come of Age. *Biotechnology advances*, 30(5):1185–1194, 2012.

[25] M Castellanos, D B Wilson, and M L Shuler. A modular minimal cell model: purine and pyrimidine transport and metabolism. *Proc Natl Acad Sci*, 101(17):6681–6, Apr 2004.

[26] Roger L. Chang, Kathleen Andrews, Donghyuk Kim, Zhanwen Li, Adam Godzik, and Bernhard O. Palsson. Structural systems biology evaluation of metabolic thermotolerance in Escherichia coli. *Science*, 340(6137):1220–1223, 2013.

[27] James Chappell, Melissa K. Takahashi, and Julius B. Lucks. Creating small transcription activating RNAs. *Nature Chemical Biology*, 11(3):214–220, March 2015.

[28] Xixian Chen, Congqiang Zhang, Ruiyang Zou, Gregory Stephanopoulos, and Heng-Phon Too. In Vitro Metabolic Engineering of Amorpha-4,11-diene Biosynthesis at Enhanced Rate and Specific Yield of Production. *ACS synthetic biology*, 6(9):1691–1700, 2017.

[29] Xixian Chen, Congqiang Zhang, Ruiyang Zou, Kang Zhou, Gregory Stephanopoulos, and Heng Phon Too. Statistical experimental design guided optimization of a one-pot biphasic multienzyme total synthesis of amorpha-4,11-diene. *PloS one*, 8(11):e79650, 2013.

[30] Daphne Collias, Ryan Marshall, Scott P Collins, Chase L Beisel, and Vincent Noireaux. An educational module to explore crispr technologies with a cell-free transcription-translation system. *Synthetic Biology*, 4(1):ysz005, 2019.

[31] Markus W Covert, Eric M Knight, Jennifer L Reed, Markus J Herrgard, and Bernhard O Palsson. Integrating high-throughput and computational data elucidates bacterial networks. *Nature*, 429(6987):92–6, May 2004.

[32] D Dai, N Horvath, and J. Varner. Dynamic Sequence Specific Constraint-Based Modeling of Cell-Free Protein Synthesis. *Processes*, 6:132, 2018.

[33] Samar Damiati, Rami Mhanna, Rimantas Kodzius, and Eva-Kathrin Ehmoser. Cell-free approaches in synthetic biology utilizing microfluidics. *Genes*, 9(3):144, 2018.

[34] Katja Dettmer, Pavel A. Aronov, and Bruce D. Hammock. Mass spectrometry-based metabolomics. *Mass Spectrometry Reviews*, 26(1):51–78, 2007.

[35] Andriy Didovyk, Taishi Tonooka, Lev Tsimring, and Jeff Hasty. Rapid and scalable preparation of bacterial lysates for cell-free gene expression. *ACS synthetic biology*, 6(12):2198–2208, 2017.

[36] M M Domach, S K Leung, R E Cahn, G G Cocks, and M L Shuler. Computer model for glucose-limited growth of a single cell of Escherichia coli b/r-a. *Biotechnol Bioeng*, 26(3):203–16, Mar 1984.

[37] Dijun Du, Hendrik W van Veen, and Ben F Luisi. Assembly and operation of bacterial tripartite multidrug efflux pumps. *Trends in Microbiology*, 23(5):311–319, 2015.

[38] Quentin M Dudley, Kim C Anderson, and Michael C Jewett. Cell-free mixing of escherichia coli crude extracts to prototype and rationally engineer high-titer mevalonate synthesis. *ACS synthetic biology*, 5(12):1578–1588, 2016.

[39] Quentin M Dudley, Ashty S Karim, and Michael C Jewett. Cell-free metabolic engineering: biomanufacturing beyond the cell. *Biotechnology journal*, 10(1):69–82, 2015.

[40] Quentin M Dudley, Connor J Nash, and Michael C Jewett. Cell-free

biosynthesis of limonene using enzyme-enriched Escherichia coli lysates. *Synthetic Biology*, 4(1):ysz003, 2019.

[41] Warwick B. Dunn, Alexander Erban, Ralf J M Weber, Darren J. Creek, Marie Brown, Rainer Breitling, Thomas Hankemeier, Royston Goodacre, Steffen Neumann, Joachim Kopka, and Mark R. Viant. Mass appeal: Metabolite identification in mass spectrometry-focused untargeted metabolomics. *Metabolomics : Official journal of the Metabolomic Society*, 9(1):44–66, 2013.

[42] Jeremy S. Edwards and Bernhard O. Palsson. Metabolic flux balance analysis and the in silico analysis of Escherichia coli k-12 gene deletions. *BMC Bioinformatics*, 1(1):1, 2000.

[43] Mary Ann A. Endoma-Arias, D. Phillip Cox, and Tomas Hudlicky. General Method of Synthesis for Naloxone, Naltrexone, Nalbuphone, and Nalbuphine by the Reaction of Grignard Reagents with an Oxazolidine Derived from Oxymorphone. *Advanced Synthesis & Catalysis*, 355(9):1869–1873, 2013.

[44] Elena Fossati, Andrew Ekins, Lauren Narcross, Yun Zhu, Jean-Pierre Falgueyret, Guillaume A. W. Beaudoin, Peter J Facchini, and Vincent J. J. Martin. Reconstitution of a 10-gene pathway for synthesis of the plant alkaloid dihydrosanguinarine in saccharomyces cerevisiae. *Nat Commun*, 5, 02 2014.

[45] A G Fredrickson. Formulation of structured growth models. *Biotechnol Bioeng*, 18(10):1481–6, Oct 1976.

[46] Brian R Fritz and Michael C Jewett. The impact of transcriptional tuning on in vitro integrated rrna transcription and ribosome construction. *Nucleic acids research*, 42(10):6774–6785, 2014.

[47] Ernest F Gale and Joan P Folkes. Effect of nucleic acids on protein synthesis and amino-acid incorporation in disrupted staphylococcal cells. *Nature*, 173:1223–7, 1954.

[48] Jonathan Garamella, Ryan Marshall, Mark Rustad, and Vincent Noireaux. The all e. coli tx-tl toolbox 2.0: A platform for cell-free synthetic biology. *ACS Synth Biol*, 5(4):344–55, Apr 2016.

[49] David Garenne and Vincent Noireaux. Cell-free transcription–translation:

engineering biology from the nanometer to the millimeter scale. *Current Opinion in Biotechnology*, 58:19–27, 2019.

[50] V. Georgi, L. Georgi, M. Blechert, M. Bergmeister, M. Zwanzig, D. A. Wüstenhagen, F. F. Bier, E. Jung, and S. Kubick. On-chip automation of cell-free protein synthesis: new opportunities due to a novel reaction mode. *Lab on a Chip*, 16(2):269–281, January 2016.

[51] Belay Gessesse, Takashi Nagaike, Koji Nagata, Yoshihiro Shimizu, and Takuya Ueda. G-protein coupled receptor protein synthesis on a lipid bilayer using a reconstituted cell-free protein synthesis system. *Life*, 8(4):54, 2018.

[52] Maximilian Glettenberg and Christof M. Niemeyer. Tuning of Peroxidase Activity by Covalently Tethered DNA Oligonucleotides. *Bioconjugate Chemistry*, 20(5):969–975, May 2009. Publisher: American Chemical Society.

[53] Aaron R. Goerke and James R. Swartz. Development of cell-free protein synthesis platforms for disulfide bonded proteins. *Biotechnol Bioeng*, 99(2):351–367, 2008.

[54] Alexander Gräwe, Anna Dreyer, Tobias Vornholt, Ursela Barteczko, Luzia Buchholz, Gila Drews, Uyen Linh Ho, Marta Eva Jackowski, Melissa Kracht, Janina Lüders, et al. A paper-based, cell-free biosensor system for the detection of heavy metals and date rape drugs. *PLoS one*, 14(3):e0210940, 2019.

[55] Nicole E Gregorio, Max Z Levine, and Javin P Oza. A user's guide to cell-free protein synthesis. *Methods and Protocols*, 2(1):24, 2019.

[56] Cassandra Guarino and Matthew P DeLisa. A prokaryote-based cell-free translation system that efficiently synthesizes glycoproteins. *Glycobiology*, 22(5):596–601, May 2012.

[57] Weihua Guo, Jiayuan Sheng, and Xueyang Feng. Mini-review: In vitro metabolic engineering for biomanufacturing of high-value products. *Computational and Structural Biotechnology Journal*, 15:161 – 167, 2017.

[58] Ravi Gupta, Nilay D. Shah, and Joseph S. Ross. The Rising Price of Naloxone — Risks to Efforts to Stem Overdose Deaths. *New England Journal of Medicine*, 375(23):2213–2215, December 2016.

[59] Jan-Karl Guterl, Daniel Garbe, Jörg Carsten, Fabian Steffler, Bettina Sommer, Steven Reiße, Anja Philipp, Martina Haack, Broder Rühmann, Andre Koltermann, Kettling Ulrich, Thomas Brück, and Volker Sieber. Cell-free metabolic engineering: production of chemicals by minimized reaction cascades. *ChemSusChem*, 5(11):2165–2172, 2012.

[60] A. Gyorgy and R. M. Murray. Quantifying resource competition and its effects in the TX-TL system. In *2016 IEEE 55th Conference on Decision and Control (CDC)*, pages 3363–3368, December 2016.

[61] H Hajjaj, P.J Blanc, G Goma, and J François. Sampling techniques and comparative extraction procedures for quantitative determination of intra- and extracellular metabolites in filamentous fungi. *FEMS Microbiology Letters*, 164(1):195–200, 1998.

[62] Shogo Hamada, Kenneth Gene Yancey, Yehudah Pardo, Mingzhe Gan, Max Vanatta, Duo An, Yue Hu, Thomas L. Derrien, Roanna Ruiz, Peifeng Liu, Jenny Sabin, and Dan Luo. Dynamic dna material with emergent locomotion behavior powered by artificial metabolism. *Science Robotics*, 4(29), 2019.

[63] Joshua J Hamilton, Vivek Dwivedi, and Jennifer L Reed. Quantitative Assessment of Thermodynamic Constraints on the Solution Space of Genome-Scale Metabolic Models. *Biophys J*, 105(2):512–522, Jul 2013.

[64] Ryan L. Hartman, Jonathan P. McMullen, and Klavs F. Jensen. Deciding Whether To Go with the Flow: Evaluating the Merits of Flow Reactors for Synthesis. *Angewandte Chemie International Edition*, 50(33):7502–7519, 2011.

[65] Sueko Hayashi and Satoshi Nakamura. Multiple forms of glucose oxidase with different carbohydrate compositions. *Biochimica et Biophysica Acta (BBA) - Enzymology*, 657(1):40–51, January 1981.

[66] Christopher S Henry, Linda J Broadbelt, and Vassily Hatzimanikatis. Thermodynamics-Based Metabolic Flux Analysis. *Biophys. J*, 92(5):192–1805, Mar 2006.

[67] Jason R Hillebrecht and Shaorong Chong. A comparative study of protein synthesis in in vitro systems: from the prokaryotic reconstituted to the eukaryotic extract-based. *BMC biotechnology*, 8(1):58, 2008.

[68] Mahlon B Hoagland, Elizabeth B Keller, and Paul C Zamecnik. Enzymatic carboxyl activation of amino acids. *J Biol Chem*, 218(1):345–358, 1956.

[69] C Eric Hodgman and Michael C Jewett. Cell-free synthetic biology: thinking outside the cell. *Metab Eng*, 14(3):261–9, May 2012.

[70] Peter-John Holt, Neil C. Bruce, and Christopher R. Lowe. Bioluminescent Assay for Heroin and Its Metabolites. *Analytical Chemistry*, 68(11):1877–1882, January 1996.

[71] Nicholas Horvath, Michael Vilkhovoy, Joseph A. Wayman, Kara Calhoun, James Swartz, and Jeffrey D. Varner. Toward a genome scale sequence specific dynamic model of cell-free protein synthesis in Escherichia coli. *Metab. Eng. Comm*, 10:e00113, 2020.

[72] Chelsea Y Hu, Jeffrey D Varner, and Julius B Lucks. Generating effective models and parameters for rna genetic circuits. *ACS Synth Biol*, 4(8):914–26, Aug 2015.

[73] Tianjiao Huang, Michael R. Armbruster, John B. Coulton, and James L. Edwards. Chemical tagging in mass spectrometry for systems biology. *Analytical Chemistry*, 91(1):109–125, Jan 2019.

[74] Tianjiao Huang, Maria Toro, Richard Lee, Dawn S. Hui, and James L. Edwards. Multi-functional derivatization of amine, hydroxyl, and carboxylate groups for metabolomic investigations of human tissue by electrospray ionization mass spectrometry. *Analyst*, 143:3408–3414, 2018.

[75] Keitaro Ishikawa, Kanetomo Sato, Yasufumi Shima, Itaru Urabe, and Tetsuya Yomo. Expression of a cascading genetic network within liposomes. *FEBS letters*, 576(3):387–390, 2004.

[76] Kirsten Jackson, Shouguang Jin, and Z Hugh Fan. Optimization of a miniaturized fluid array device for cell-free protein synthesis. *Biotechnol Bioeng*, 112(12):2459–2467, 2015.

[77] Amber Jannasch, Miroslav Sedlak, and Jiri Adamec. Quantification of pentose phosphate pathway (ppp) metabolites by liquid chromatography-mass spectrometry (lc-ms). *Methods in molecular biology (Clifton, N.J.)*, 708:159–171, 2011.

[78] Amber Jannasch, Miroslav Sedlak, and Jiri Adamec. Quantifica-

tion of Pentose Phosphate Pathway (PPP) Metabolites by Liquid Chromatography-Mass Spectrometry (LC-MS). In Thomas O. Metz, editor, *Metabolic Profiling: Methods and Protocols*, pages 159–171. Humana Press, Totowa, NJ, 2011.

[79] Thapakorn Jaroentomeechai, Jessica C Stark, Aravind Natarajan, Cameron J Glasscock, Laura E Yates, Karen J Hsu, Milan Mrksich, Michael C Jewett, and Matthew P DeLisa. Single-pot glycoprotein biosynthesis using a cell-free transcription-translation system enriched with glycosylation machinery. *Nature communications*, 9(1):2686, 2018.

[80] Michael C Jewett, Kara A Calhoun, Alexei Voloshin, Jessica J Wuu, and James R Swartz. An integrated cell-free metabolic platform for protein production and synthetic biology. *Mol Syst Biol*, 4:220, 2008.

[81] Michael C Jewett, Brian R Fritz, Laura E Timmerman, and George M Church. In vitro integration of ribosomal RNA synthesis, ribosome assembly, and translation. *Molecular Systems Biology*, 9(1):678, 2013.

[82] Michael C. Jewett and James R. Swartz. Mimicking the Escherichia coli cytoplasmic environment activates long-lived and efficient cell-free protein synthesis. *Biotechnol Bioeng*, 86(1):19–26, 2004.

[83] Michael C. Jewett and James R. Swartz. Substrate replenishment extends protein synthesis with an in vitro translation system designed to mimic the cytoplasm. *Biotechnol Bioeng*, 87(4):465–471, 2004.

[84] H. M. Kalisz, J. Hendle, and R. D. Schmid. Structural and biochemical properties of glycosylated and deglycosylated glucose oxidase from Penicillium amagasakiense. *Applied Microbiology and Biotechnology*, 47(5):502–507, May 1997.

[85] David K Karig, Sukanya Iyer, Michael L Simpson, and Mitchel J Doktycz. Expression optimization and synthetic gene networks in cell-free systems. *Nucleic acids research*, 40(8):3763–3774, 2011.

[86] J. R. Karr, J. C. Sanghvi, D. N. Macklin, M. V. Gutschow, J. M. Jacobs, B. Bolival, N. Assad-Garcia, J. I. Glass, and M. W. Covert. A whole-cell computational model predicts phenotype from genotype. *Cell*, 150(2):389–401, Jul 2012.

[87] Eyal Karzbrun, Jonghyeon Shin, Roy H. Bar-Ziv, and Vincent Noireaux.

Coarse-Grained Dynamics of Protein Synthesis in a Cell-Free System. *Physical Review Letters*, 106(4), January 2011.

[88] Eyal Karzbrun, Alexandra M Tayar, Vincent Noireaux, and Roy H Bar-Ziv. Programmable on-chip dna compartments as artificial cells. *Science*, 345(6198):829–832, 2014.

[89] Takanori Kigawa, Takashi Yabuki, Natsuko Matsuda, Takayoshi Matsuda, Rie Nakajima, Akiko Tanaka, and Shigeyuki Yokoyama. Preparation of escherichia coli cell extract for highly productive cell-free protein expression. *Journal of structural and functional genomics*, 5(1-2):63–68, 2004.

[90] Dong-Myung Kim and James R. Swartz. Regeneration of adenosine triphosphate from glycolytic intermediates for cell-free protein synthesis. *Biotechnol Bioeng*, 74(4):309–316, 2001.

[91] Dong-Myung Kim and James R Swartz. Regeneration of adenosine triphosphate from glycolytic intermediates for cell-free protein synthesis. *Biotechnol Bioeng*, 74(4):309–316, 2001.

[92] Tae-Wan Kim, Jung-Won Keum, In-Seok Oh, Cha-Yong Choi, Chang-Gil Park, and Dong-Myung Kim. Simple procedures for the construction of a robust and cost-effective cell-free protein synthesis system. *Journal of biotechnology*, 126(4):554–561, 2006.

[93] Gordana Kovačević, Marija Blažić, Bojana Draganić, Raluca Ostafe, Marija Gavrović-Jankulović, Rainer Fischer, and Radivoje Prodanović. Cloning, Heterologous Expression, Purification and Characterization of M12 Mutant of Aspergillus niger Glucose Oxidase in Yeast Pichia pastoris KM71H. *Molecular Biotechnology*, 56(4):305–311, April 2014.

[94] Borimas Krutsakorn, Kohsuke Honda, Xiaoting Ye, Takashi Imagawa, Xiaoyu Bei, Kenji Okano, and Hisao Ohtake. In vitro production of n-butanol from glucose. *Metabolic engineering*, 20:84–91, 2013.

[95] Muriel Lederman and Geoffrey Zubay. Dna-directed peptide synthesis i. a comparison of t2 and Escherichia coli dna-directed peptide synthesis in two cell-free systems. *Biochimica et Biophysica Acta (BBA)-Nucleic Acids and Protein Synthesis*, 149(1):253–258, 1967.

[96] Nathan E Lewis, Harish Nagarajan, and Bernhard Ø Palsson. Constraining the metabolic genotype-phenotype relationship using a phylogeny of in silico methods. *Nat Rev Microbiol*, 10(4):291–305, Apr 2012.

[97] Jun Li, Liangcai Gu, John Aach, and George M Church. Improved cell-free rna and protein synthesis system. *PLoS one*, 9(9):e106232, 2014.

[98] David V Liu, James F Zawada, and James R Swartz. Streamlining escherichia coli s30 extract preparation for economical cell-free protein synthesis. *Biotechnology Progress*, 21(2):460–465, 2005.

[99] M T Long, A M Hailes, G W Kirby, and N C Bruce. Transformations of morphine alkaloids by Pseudomonas putida M10. *Applied and Environmental Microbiology*, 61(10):3645–3649, October 1995.

[100] Yuan Lu, John P Welsh, and James R Swartz. Production and stabilization of the trimeric influenza hemagglutinin stem domain for potentially broadly protective influenza vaccines. *Proc Natl Acad Sci*, 111(1):125–30, Jan 2014.

[101] Julius B. Lucks, Lei Qi, Vivek K. Mutalik, Denise Wang, and Adam P. Arkin. Versatile RNA-sensing transcriptional regulators for engineering genetic networks. *Proc Natl Acad Sci*, 108(21):8617–8622, May 2011.

[102] Duo Ma, Luhui Shen, Kaiyue Wu, Chris W Diehnelt, and Alexander A Green. Low-cost detection of norovirus using paper-based cell-free systems and synbody-based viral enrichment. *Synthetic Biology*, 3(1):ysy018, 2018.

[103] Rey W Martin, Benjamin J Des Soye, Yong-Chan Kwon, Jennifer Kay, Roderick G Davis, Paul M Thomas, Natalia I Majewska, Cindy X Chen, Ryan D Marcum, Mary Grace Weiss, et al. Cell-free protein synthesis from genomically recoded bacteria enables multisite incorporation of noncanonical amino acids. *Nature communications*, 9(1):1203, 2018.

[104] Laura Martini and Sheref S Mansy. Measuring riboswitch activity in vitro and in artificial cells with purified transcription–translation machinery. In *Artificial Riboswitches*, pages 153–164. Springer, 2014.

[105] J H Matthaei and M W Nirenberg. Characteristics and stabilization of dnaase-sensitive protein synthesis in e. coli extracts. *Proc Natl Acad Sci*, 47:1580–8, Oct 1961.

[106] Doreen Matthies, Stefan Haberstock, Friederike Joos, Volker Dötsch, Janet Vonck, Frank Bernhard, and Thomas Meier. Cell-free expression and assembly of atp synthase. *Journal of Molecular Biology*, 413(3):593–603, 2011.

[107] D. Tyler McQuade and Peter H. Seeberger. Applying Flow Chemistry: Methods, Materials, and Multistep Synthesis. *The Journal of Organic Chemistry*, 78(13):6384–6389, July 2013.

[108] Nathalie Michel-Reydellet, Kara Calhoun, and James Swartz. Amino acid stabilization for cell-free protein synthesis by modification of the escherichia coli genome. *Metabolic engineering*, 6(3):197–203, 2004.

[109] Seung Eui Min, Kyung-Ho Lee, Seong-Wook Park, Tae Hyeon Yoo, Chan Hee Oh, Ji-Ho Park, Sung Yun Yang, Yong-Sung Kim, and Dong-Myung Kim. Cell-free production and streamlined assay of cytosol-penetrating antibodies. *Biotechnology and bioengineering*, 113(10):2107–12, 2016.

[110] Simon J Moore, James T MacDonald, Sarah Wienecke, Alka Ishwarbhai, Argyro Tsipa, Rochelle Aw, Nicolas Kylilis, David J Bell, David W McClymont, Kirsten Jensen, et al. Rapid acquisition and model-based analysis of cell-free transcription–translation reactions from nonmodel bacteria. *Proceedings of the National Academy of Sciences*, 115(19):E4340–E4349, 2018.

[111] H J Morowitz. The completeness of molecular biology. *Isr J Med Sci*, 20(9):750–3, Sep 1984.

[112] Satoshi Murakami, Rena Matsumoto, and Takashi Kanamori. Constructive approach for synthesis of a functional IgG using a reconstituted cell-free protein synthesis system. *Scientific Reports*, 9(1):1–13, 2019.

[113] Travis W Murphy, Jiayuan Sheng, Lynette B Naler, Xueyang Feng, and Chang Lu. On-chip manufacturing of synthetic proteins for point-of-care therapeutics. *Microsystems & nanoengineering*, 5(1):1–12, 2019.

[114] Charles E Nakamura and Gregory M Whited. Metabolic engineering for the microbial production of 1,3-propanediol. *Current Opinion in Biotechnology*, 14(5):454 – 459, 2003.

[115] Satoshi Nakamura, Sueko Hayashi, and Kunimasa Koga. Effect of periodate oxidation on the structure and properties of glucose oxidase. *Biochimica et Biophysica Acta (BBA) - Enzymology*, 445(2):294–308, September 1976.

[116] Aravind Natarajan, Thapakorn Jaroentomeechai, Marielisa Cabrera-Sánchez, Jody C. Mohammed, Emily C. Cox, Olivia Young, Asif Shajahan, Michael Vilkhovoy, Sandra Vadhin, Jeffrey D. Varner, Parastoo Azadi, and

Matthew P. DeLisa. Engineering orthogonal human O- linked glycoprotein biosynthesis in bacteria. *Nature Chemical Biology*, 16(10):1062–1070, October 2020. Number: 10 Publisher: Nature Publishing Group.

[117] Patrick P Ng, Ming Jia, Kedar G Patel, Joshua D Brody, James R Swartz, Shoshana Levy, and Ronald Levy. A vaccine directed to b cells and produced by cell-free protein synthesis generates potent antilymphoma immunity. *Proc Natl Acad Sci*, 109(36):14526–14531, 2012.

[118] Pamela N. Nge, Chad I. Rogers, and Adam T. Woolley. Advances in Microfluidic Materials, Functions, Integration, and Applications. *Chemical Reviews*, 113(4):2550–2583, April 2013.

[119] Henrike Niederholtmeyer, Zachary Z Sun, Yutaka Hori, Enoch Yeung, Amanda Verpoorte, Richard M Murray, and Sebastian J Maerkl. Rapid cell-free forward engineering of novel genetic ring oscillators. *Elife*, 4:e09771, 2015.

[120] Henrike Niederholtmeyer, Ling Xu, and Sebastian J Maerkl. Real-time mrna measurement during an in vitro transcription and translation reaction using binary probes. *ACS synthetic biology*, 2(8):411–417, 2012.

[121] Alexander Nieß, Jurek Failmezger, Maike Kuschel, Martin Siemann-Herzberg, and Ralf Takors. Experimentally Validated Model Enables Debottlenecking of in Vitro Protein Synthesis and Identifies a Control Shift under in Vivo Conditions. *ACS Synthetic Biology*, 6(10):1913–1921, October 2017.

[122] M W Nirenberg and J H Matthaei. The dependence of cell-free protein synthesis in e. coli upon naturally occurring or synthetic polyribonucleotides. *Proc Natl Acad Sci*, 47:1588–602, Oct 1961.

[123] Marshall W. Nirenberg and J. Heinrich Matthaei. The dependence of cell-free protein synthesis in E. coli upon naturally occurring or synthetic polyribonucleotides. *Proceedings of the National Academy of Sciences*, 47(10):1588–1602, 1961.

[124] Tatsuya Niwa, Yoshihiro Sasaki, Eri Uemura, Shugo Nakamura, Minato Akiyama, Mitsuru Ando, Shinichi Sawada, Sada-atu Mukai, Takuya Ueda, Hideki Taguchi, et al. Comprehensive study of liposome-assisted synthesis of membrane proteins using a reconstituted cell-free translation system. *Scientific reports*, 5:18025, 2015.

[125] Vincent Noireaux and Albert Libchaber. A vesicle bioreactor as a step toward an artificial cell assembly. *Proc Natl Acad Sci*, 101(51):17669–17674, 2004.

[126] Edward J O'Brien, Joshua A Lerman, Roger L Chang, Daniel R Hyduke, and Bernhard Ø Palsson. Genome-scale models of metabolism and gene expression extend and refine growth phenotype prediction. *Mol. Sys. Biol.*, 9(1):693, 2013.

[127] Olotu W Ogonah, Karen M Polizzi, and Daniel G Bracewell. Cell free protein synthesis: a viable option for stratified medicines manufacturing? *Current Opinion in Chemical Engineering*, 18:77–83, 2017.

[128] Paul H Opgenorth, Tyler P Korman, and James U Bowie. A synthetic biochemistry molecular purge valve module that maintains redox balance. *Nature communications*, 5:4113, 2014.

[129] Paul H Opgenorth, Tyler P Korman, and James U Bowie. A synthetic biochemistry module for production of bio-based chemicals from glucose. *Nature Chemical Biology*, 12(6):393–395, 2016.

[130] Keith Pardee, Alexander A Green, Tom Ferrante, D Ewen Cameron, Ajay DaleyKeyser, Peng Yin, and James J Collins. Paper-based synthetic gene networks. *Cell*, 159(4):940–954, 2014.

[131] Keith Pardee, Alexander A Green, Melissa K Takahashi, Dana Braff, Guillaume Lambert, Jeong Wook Lee, Tom Ferrante, Duo Ma, Nina Donghia, Melina Fan, et al. Rapid, low-cost detection of zika virus using programmable biomolecular components. *Cell*, 165(5):1255–1266, 2016.

[132] Keith Pardee, Shimyn Slomovic, Peter Q Nguyen, Jeong Wook Lee, Nina Donghia, Devin Burrill, Tom Ferrante, Fern R McSorley, Yoshikazu Furuta, Andyna Vernet, Michael Lewandowski, Christopher N Boddy, Neel S Joshi, and James J Collins. Portable, on-demand biomolecular manufacturing. *Cell*, 167(1):248–59.e12, Sep 2016.

[133] Tereza Pereira de Souza, Pasquale Stano, and Pier Luigi Luisi. The minimal size of liposome-based model cells brings about a remarkably enhanced entrapment and protein synthesis. *ChemBioChem*, 10(6):1056–1063, 2009.

[134] Jessica G Perez, Jessica C Stark, and Michael C Jewett. Cell-free synthetic

biology: engineering beyond the cell. *Cold Spring Harbor perspectives in biology*, 8(12):a023853, 2016.

[135] JM Pratt. Coupled transcription-translation in prokaryotic cell-free systems. *Transcription and translation: a practical approach.*, pages 179–209, 1984.

[136] JI Qiu, James R Swartz, and George Georgiou. Expression of active human tissue-type plasminogen activator in escherichia coli. *Appl. Environ. Microbiol.*, 64(12):4891–4896, 1998.

[137] Deborah A. Rathbone, Peter-John Holt, Christopher R. Lowe, and Neil C. Bruce. The Use of a Novel Recombinant Heroin Esterase in the Development of an Illicit Drugs Biosensora. *Annals of the New York Academy of Sciences*, 799(1):90–96, 1996.

[138] Dae-Kyun Ro, Eric M Paradise, Mario Ouellet, Karl J Fisher, Karyn L Newman, John M Ndungu, Kimberly A Ho, Rachel A Eachus, Timothy S Ham, James Kirby, Michelle C Y Chang, Sydnor T Withers, Yoichiro Shiba, Richmond Sarpong, and Jay D Keasling. Production of the antimalarial drug precursor artemisinic acid in engineered yeast. *Nature*, 440(7086):940–3, Apr 2006.

[139] Gabriel Rosenblum and Barry S. Cooperman. Engine out of the chassis: Cell-free protein synthesis and its uses. *FEBS Letters*, 588(2):261 – 268, 2014. Protein Engineering.

[140] G.J.G. Ruijter and J. Visser. Determination of intermediary metabolites in aspergillus niger. *Journal of Microbiological Methods*, 25(3):295 – 302, 1996.

[141] Rachael Rzasa Lynn and Jl Galinkin. Naloxone dosage for opioid reversal: current evidence and clinical implications. *Therapeutic Advances in Drug Safety*, 9(1):63–88, January 2018.

[142] Ryota Sakamoto, Vincent Noireaux, and Yusuke T Maeda. Anomalous scaling of gene expression in confined cell-free reactions. *Scientific reports*, 8(1):7364, 2018.

[143] Amin S M Salehi, Mark Thomas Smith, Anthony M Bennett, Jacob B Williams, William G Pitt, and Bradley C Bundy. Cell-free protein synthesis of a cytotoxic cancer therapeutic: Onconase production and a just-add-water cell-free system. *Biotechnology Journal*, 11(2):274–281, 2015.

[144] Claudia Sánchez, Juan Carlos Quintero, and Silvia Ochoa. Flux balance analysis in the production of clavulanic acid by Streptomyces clavuligerus. *Biotechnol Prog*, 31(5):1226–1236, 2015.

[145] C H Schilling, D Letscher, and B O Palsson. Theory for the systemic definition of metabolic pathways and their use in interpreting metabolic function from a pathway-oriented perspective. *J Theor Biol*, 203(3):229–48, Apr 2000.

[146] S Schuster, D A Fell, and T Dandekar. A general definition of metabolic pathways useful for systematic organization and analysis of complex metabolic networks. *Nat Biotechnol*, 18(3):326–32, Mar 2000.

[147] Yoshihiro Shimizu, Akio Inoue, Yukihide Tomari, Tsutomu Suzuki, Takashi Yokogawa, Kazuya Nishikawa, and Takuya Ueda. Cell-free translation reconstituted with purified components. *Nature biotechnology*, 19(8):751, 2001.

[148] Jonghyeon Shin and Vincent Noireaux. Efficient cell-free expression with the endogenous e. coli rna polymerase and sigma factor 70. *J Biol Eng*, 4:8, Jun 2010.

[149] Jonghyeon Shin and Vincent Noireaux. Study of messenger RNA inactivation and protein degradation in an Escherichia coli cell-free expression system. *Journal of Biological Engineering*, 4(1):9, July 2010.

[150] Jonghyeon Shin and Vincent Noireaux. An e. coli cell-free expression toolbox: application to synthetic gene circuits and artificial cells. *ACS synthetic biology*, 1(1):29–41, 2012.

[151] Takehiro Shinoda, Naoko Shinya, Kaori Ito, Yoshiko Ishizuka-Katsura, Noboru Ohsawa, Takaho Terada, Kunio Hirata, Yoshiaki Kawano, Masaki Yamamoto, Taisuke Tomita, et al. Cell-free methods to produce structurally intact mammalian membrane proteins. *Scientific reports*, 6:30442, 2016.

[152] Prashanta Shrestha, Troy Michael Holland, and Bradley Charles Bundy. Streamlined extract preparation for escherichia coli-based cell-free protein synthesis by sonication or bead vortex mixing. *Biotechniques*, 53(3):163–174, 2012.

[153] Adam D Silverman, Ashty S Karim, and Michael C Jewett. Cell-free gene

expression: an expanded repertoire of applications. *Nature Reviews Genetics*, pages 1–20, 2019.

[154] Adam D Silverman, Nancy Kelley-Loughnane, Julius B Lucks, and Michael C Jewett. Deconstructing cell-free extract preparation for in vitro activation of transcriptional genetic circuitry. *ACS synthetic biology*, 8(2):403–414, 2018.

[155] C. Simpson, J. Jordaan, N. S. Gardiner, and C. Whiteley. Isolation, purification and characterization of a novel glucose oxidase from Penicillium sp. CBS 120262 optimally active at neutral pH. *Protein Expression and Purification*, 51(2):260–266, February 2007.

[156] Mark Thomas Smith, Anthony M Bennett, Jeremy M Hunt, and Bradley C Bundy. Creating a completely "cell-free" system for protein synthesis. *Biotechnology Progress*, 31(6):1716–1719, 2015.

[157] Helen Song, Michelle R. Bringer, Joshua D. Tice, Cory J. Gerdts, and Rustem F. Ismagilov. Experimental test of scaling of mixing by chaotic advection in droplets moving through microfluidic channels. *Applied physics letters*, 83(12):4664–4666, December 2003.

[158] Hyohak Song and Sang Yup Lee. Production of succinic acid by bacterial fermentation. *Enzyme and Microbial Technology*, 39(3):352 – 361, 2006. The Asia-Pacific Biochemical Engineering Conference (APBioChEC 2005).

[159] AS Spirin, VI Baranov, LA Ryabova, SY Ovodov, and YB Alakhov. A continuous cell-free translation system capable of producing polypeptides in high yield. *Science*, 242(4882):1162–1164, 1988.

[160] Jessica C Stark, Thapakorn Jaroentomeechai, Tyler D Moeller, Rachel S Dubner, Karen J Hsu, Taylor C Stevenson, Matthew P DeLisa, and Michael C Jewett. On-demand, cell-free biomanufacturing of conjugate vaccines at the point-of-care. *bioRxiv*, page 681841, 2019.

[161] D.E. Steinmeyer and M.L. Shuler. Structured model for Saccharomyces cerevisiae. *Chem. Eng. Sci.*, 44:2017–2030, 1989.

[162] Tobias Stögbauer, Lukas Windhager, Ralf Zimmer, and Joachim O. Rädler. Experiment and mathematical modeling of gene expression dynamics in a cell-free system. *Integrative Biology*, 4(5):494–501, May 2012.

[163] James R. Swartz. Expanding biological applications using cell-free metabolic engineering: An overview. *Metabolic Engineering*, 50(October):156–172, 2018.

[164] Jim Swartz. Developing cell-free biology for industrial applications. *Journal of Industrial Microbiology and Biotechnology*, 33(7):476–485, 2006.

[165] Jim Swartz. Developing cell-free biology for industrial applications. *Journal of Industrial Microbiology and Biotechnology*, 33(7):476–485, July 2006.

[166] Kazuyuki Takai, Tatsuya Sawasaki, and Yaeta Endo. Practical cell-free protein synthesis system using purified wheat embryos. *Nature Protocols*, 5, 2001.

[167] K. Takegawa, K. Fujiwara, S. Iwahara, K. Yamamoto, and T. Tochikura. Effect of deglycosylation of N-linked sugar chains on glucose oxidase from Aspergillus niger. *Biochemistry and cell biology = Biochimie et biologie cellulaire*, 67(8):460–464, January 1989. Publisher: National Research Council of Canada.

[168] Alexandra M Tayar, Eyal Karzbrun, Vincent Noireaux, and Roy H Bar-Ziv. Synchrony and pattern formation of coupled genetic oscillators on a chip of artificial cells. *Proc Natl Acad Sci*, 114(44):11609–11614, 2017.

[169] Uwe Theobald, Werner Mailinger, Michael Baltes, Manfred Rizzi, and Matthias Reuss. In vivo analysis of metabolic dynamics in saccharomyces cerevisiae : I. experimental observations. *Biotechnol Bioeng*, 55(2):305–316, 1997.

[170] Ines Thiele, Neema Jamshidi, Ronan M. T. Fleming, and Bernhard O. Palsson. Genome-scale reconstruction of Escherichia coli's transcriptional and translational machinery: A knowledge base, its mathematical formulation, and its functional characterization. *PLOS Computational Biology*, 5(3):1–13, 03 2009.

[171] Andrea C Timm, Peter G Shankles, Carmen M Foster, Mitchel J Doktycz, and Scott T Retterer. Toward microfluidic reactors for cell-free protein synthesis at the point-of-care. *Small*, 12(6):810–817, 2016.

[172] M Tomita, K Hashimoto, K Takahashi, T S Shimizu, Y Matsuzaki, F Miyoshi, K Saito, S Tanida, K Yugi, J C Venter, and C A Hutchison. E-cell: software environment for whole-cell simulation. *Bioinformatics*, 15(1):72–84, 1999.

[173] Meaghan A Valliere, Tyler P Korman, Nicholas B Woodall, Gregory A Khitrov, Robert E Taylor, David Baker, and James U Bowie. A cell-free platform for the prenylation of natural products and application to cannabinoid production. *Nature Communications*, 10(1):565, 2019.

[174] A Varma and B O Palsson. Stoichiometric flux balance models quantitatively predict growth and metabolic by-product secretion in wild-type Escherichia coli W3110. *Appl. Environ. Microbiol.*, 60(10):3724–3731, 1994.

[175] M. Vilkhovoy, M. Minot, and J. D. Varner. Effective dynamic models of metabolic networks. *IEEE Life Sciences Letters*, 2(4):51–54, Dec 2016.

[176] Michael Vilkhovoy, David Dai, Sandra Vadhin, Abhinav Adhikari, and Jeffrey D Varner. Absolute quantification of cell-free protein synthesis metabolism by reversed-phase liquid chromatography-mass spectrometry. *J Vis Exp*, (152), Oct 2019.

[177] Michael Vilkhovoy, David Dai, Sandra Vadhin, Abhinav Adhikari, and Jeffrey D. Varner. Absolute Quantification of Cell-Free Protein Synthesis Metabolism by Reversed-Phase Liquid Chromatography-Mass Spectrometry. *Journal of Visualized Experiments*, (152):60329, October 2019.

[178] Michael Vilkhovoy, Nicholas Horvath, Che-Hsiao Shih, Joseph A. Wayman, Kara Calhoun, James Swartz, and Jeffrey D. Varner. Sequence specific modeling of e. coli cell-free protein synthesis. *ACS Synthetic Biology*, 7(8):1844–1857, Aug 2018.

[179] Michael Vilkhovoy, Nicholas Horvath, Che-Hsiao Shih, Joseph A. Wayman, Kara Calhoun, James Swartz, and Jeffrey D. Varner. Sequence Specific Modeling of *E. coli* Cell-Free Protein Synthesis. *ACS Synthetic Biology*, 7(8):1844–1857, August 2018.

[180] Alexei M Voloshin and James R Swartz. Efficient and scalable method for scaling up cell free protein synthesis in batch mode. *Biotechnol Bioeng*, 91(4):516–21, Aug 2005.

[181] Xiaoqiang Wang, Karolina Corin, Philipp Baaske, Christoph J Wienken, Moran Jerabek-Willemsen, Stefan Duhr, Dieter Braun, and Shuguang Zhang. Peptide surfactants for cell-free production of functional g protein-coupled receptors. *Proc Natl Acad Sci*, 108(22):9049–9054, 2011.

[182] Kevin Ward and Z Hugh Fan. Mixing in microfluidic devices and en-

hancement methods. *Journal of micromechanics and microengineering : structures, devices, and systems*, 25(9), September 2015.

[183] Joseph A. Wayman, Adithya Sagar, and Jeffrey D. Varner. Dynamic modeling of cell-free biochemical networks using effective kinetic models. *Processes*, 3(1):138, 2015.

[184] John P Welsh, Yuan Lu, Xiao-Song He, Harry B Greenberg, and James R Swartz. Cell-free production of trimeric influenza hemagglutinin head domain proteins as vaccine antigens. *Biotechnol Bioeng*, 109(12):2962–2969, 2012.

[185] Wolfgang Wiechert. 13C Metabolic Flux Analysis. *Metabol. Eng.*, 3(3):195 – 206, 2001.

[186] T Winnick. Incorporation of labeled amino acids into the protein of embryonic and tumor tissue homogenates. *Federation Proceedings*, 9(1):247, 1950.

[187] P Wu, N G Ray, and M L Shuler. A single-cell model for cho cells. *Ann N Y Acad Sci*, 665:152–87, Oct 1992.

[188] Wen-Chu Yang, Miroslav Sedlak, Fred E. Regnier, Nathan Mosier, Nancy Ho, and Jiri Adamec. Simultaneous quantification of metabolites involved in central carbon and energy metabolism using reversed-phase liquid chromatography-mass spectrometry and in vitro 13c labeling. *Analytical Chemistry*, 80(24):9508–9516, Dec 2008.

[189] Tong Yi, Hye Jin Lim, So Jeong Lee, Kyung-Ho Lee, and Dong-Myung Kim. Synthesis of (R,R)-2,3-butanediol from starch in a hybrid cell-free reaction system. *Journal of Industrial and Engineering Chemistry*, 67:231–235, 2018.

[190] Harry Yim, Robert Haselbeck, Wei Niu, Catherine Pujol-Baxley, Anthony Burgard, Jeff Boldt, Julia Khandurina, John D Trawick, Robin E Osterhout, Rosary Stephen, Jazell Estadilla, Sy Teisan, H Brett Schreyer, Stefan Andrae, Tae Hoon Yang, Sang Yup Lee, Mark J Burk, and Stephen Van Dien. Metabolic engineering of escherichia coli for direct production of 1,4-butanediol. *Nat Chem Biol*, 7(7):445–452, 07 2011.

[191] Gang Yin, Eudean D Garces, Junhao Yang, Juan Zhang, Cuong Tran, Alexander R Steiner, Christine Roos, Sunil Bajad, Susan Hudak, Kalyani

Penta, James Zawada, Sonia Pollitt, and Christopher J Murray. Aglycosylated antibodies and antibody fragments produced in a scalable in vitro transcription-translation system. In *MAbs*, volume 4, pages 217–225. Taylor & Francis, 2012.

[192] Gang Yin and James R Swartz. Enhancing multiple disulfide bonded protein folding in a cell-free system. *Biotechnol Bioeng*, 86(2):188–195, 2004.

[193] James F Zawada, Gang Yin, Alexander R Steiner, Junhao Yang, Alpana Naresh, Sushmita M Roy, Daniel S Gold, Henry G Heinsohn, and Christopher J Murray. Microscale to manufacturing scale-up of cell-free cytokine production–a new approach for shortening protein production development timelines. *Biotechnol Bioeng*, 108(7):1570–8, Jul 2011.

[194] James F Zawada, Gang Yin, Alexander R Steiner, Junhao Yang, Alpana Naresh, Sushmita M Roy, Daniel S Gold, Henry G Heinsohn, and Christopher J Murray. Microscale to manufacturing scale-up of cell-free cytokine production–a new approach for shortening protein production development timelines. *Biotechnology and bioengineering*, 108(7):1570–1578, July 2011.

[195] Ying Zhang, Ines Thiele, Dana Weekes, Zhanwen Li, Lukasz Jaroszewski, Krzysztof Ginalski, Ashley M. Deacon, John Wooley, Scott A. Lesley, Ian A. Wilson, Bernhard Palsson, Andrei Osterman, and Adam Godzik. Three-dimensional structural view of the central metabolic network of thermotoga maritima. *Science*, 325(5947):1544–1549, 2009.

[196] Xiaoyu Zhou, Han Wu, Miao Cui, Sze Nga Lai, and Bo Zheng. Long-lived protein expression in hydrogel particles: towards artificial cells. *Chemical science*, 9(18):4275–4279, 2018.

[197] Ying Zhou, Haruichi Asahara, Eric A Gaucher, and Shaorong Chong. Reconstitution of translation from thermus thermophilus reveals a minimal set of components sufficient for protein synthesis at high temperatures and functional conservation of modern and ancient translation components. *Nucleic acids research*, 40(16):7932–7945, 2012.

[198] Zhiguang Zhu, Tsz Kin Tam, Fangfang Sun, Chun You, and Y-H Percival Zhang. A high-energy-density sugar biobattery based on a synthetic enzymatic pathway. *Nature communications*, 5:3026, 2014.

[199] Geoffrey Zubay. In vitro synthesis of protein in microbial systems. *Annual review of genetics*, 7(1):267–287, 1973.